GEOTHERMAL WELL LOGGING AND TESTING

by Pierre UNGEMACH

1. INTRODUCTION

Logging and testing of geothermal wells are essential segments of any field exploration and development strategy addressing relevant reservoir engineering and resource management issues.

They constitute in deed a too vast domain, actually the substance of numerous books, papers and manuals, to be thoroughly challenged in the framework of this presentation.

Therefore the scope of the exercise will be limited and focus instead on recalls of well logging and testing basic principles and illustrated by selected field applications the latter restricted to low to medium temperature, single phase liquid, geothermal sources and sedimentary host rock environments.

The foregoing may be regarded as a set of guide lines, whose methodology could be applied while tackling similar resource settings and development problematics.

2. OBJECTIVES OF WELL LOGGING AND TESTING

Geothermal well logging deals with three major concerns (i) reservoir exploration, (ii) reservoir development, and (iii) resource exploitation / management respectively.

- Hence logging requirements address the following headings.
- Geological framework : lithostratigraphic control, structural features
- Reservoir characterisation : geometry, location of productive layers (pay zones), hydrothermal convection, pressure /temperature/flow patterns
- Fluid properties
- Design and control of well casing/completion
- Monitoring of well integrity during exploitation

These key issues intervene downstream from former geological, hydrogeological and geophysical (mainly seismic surveys) investigations and speculations.

With respect to low enthalpy geothermal deposits, whose development is fairly recent, their reconnaissance often benefited from previous hydrocarbon drilling campaigns which provided significant well control and data bases. Such was the case of the central part of the Paris Basin. Here, data collected by oil operators, and made accessible to the Public thanks to the French mining law, were reprocessed and complemented by heat flow measurements leading to a reliable evaluation of the resource base and related resource / reserve assessments. A similar situation was encountered in Central/Eastern Europe particularly in Hungary.

Worth adding is that logging information is (i) limited to the well and its immediate surroundings, and (ii) affected by the noise induced by the drilling fluids and mud cake.

Contrary to logging well testing exhibits an investigation power extending far beyond the well face, alongside a regularising (averaging) effect smoothing the impact of local heterogeneities. It appears therefore as a relevant tool for quantifying bulk reservoir behaviour.

This stated, well testing is assigned two objectives namely (i) evaluation of well and reservoir performance, and (ii) reservoir management.

From testing are derived well deliverabilities which depend on reservoir net thickness, permeability, skin, wellbore storage, static (initial) reservoir pressure, boundary conditions and field singularities, the identified drainage model (matrix or fracture dominated, dual porosity system) and fluid rheology.

Not overlooking well monitoring during production (and injection), reservoir management is closely linked to reservoir simulation which fits single well test data and production/injection histories into a generic conceptual model to forecast future pressure/temperature patterns, temperature breakthrough times, and assess useful reservoir life.

Both well logging and testing have, in the recent years, gained increased reliability from tool technology, data acquisition and, interactive computer assisted, processing software rendering interpretation a truly rewarding exercise.

3. WELL LOGGING OVERVIEW

Logging tools fall usually into three categories, openhole, cased hole and production respectively. To simplify :

- Openhole tools are exploration oriented and deal with formation and reservoir evaluation.
- Cased hole tools aim at well (casing/cement/completion) integrity control.
- Production tools are measuring and sampling devices assisting well tests and fluid analyses.
- Exploration tools deserve a special comment. As far as lithostratigraphy, porosity and permeability are concerned there is no direct in situ assessment of these petrographic and physical parameters. Instead those are measured indirectly through other, physically related, parameters such as spontaneous potentials, resistivities, bulk densities, transit times, natural radioactivity and rock hydrogen contents.
- Other, structural and tectonic, features can be appraised via magnetic, seismo acoustic measurements and image processing applied to dips and fracture determination among others.
- Drilling / completion fluids, mud cake and invaded zone effects, illustrated in fig.1 for a water bearing layer, need to be corrected in order to release true (clean) formation figures.
- Tool to tool cross correlations (crossplots) are currently practised to improve lithological identification and porosity appraisals.
- The basic formulae, borrowed to ref (1), listed in table 1 form the driving rationale of quantitative log interpretation.
- Tool nomenclature is summarised in table 2.

TOOL DESCRIPTION

GAMMA RAY (GR)

The GR wirelinelog detects, by scintillation metering/photomultiplication, the rock natural radioactivity through radiations resulting from Uranium, Thorium and Potassium radioactive decay. The radiation is measured in API units expressed as multiples of a standard calibre. Owing to the clay high radioactive contents (K40 notably), the GR log is a reliable indicator of formation argillosity. It is therefore a relevant tool in assessing clean (sand, sandstones) levels and deriving accordingly sand/clay ratios. It appears also as a pertinent lithology tool due to its ability to identify, under the form of individualized peaks, the signature of brief organic episodes, in deed useful markers in exercising lithostratigraphic correlations from well to well.

SPONTANEOUS (SELF) POTENTIAL (SP)

The SP log measures, in a well filled with a conductive mud, the electrical potential between an in hole located electrode and the surface. It therefore helps in discriminating pervious layers from clay streaks.

The SP signal originates from currents generated by the salinity contrast between the mud filtrate and the formation water. It includes an electrochemical potential and an electrofiltration potential. The first consists chiefly of a membrane potential associated to Na ion migration resulting from a gradient in concentration particularily in the case of a clay/saline brine contact. The electrofiltration potential is a consequence of electrolyte displacement in a porous medium.

Summing up, SP is a tool measuring the resistivity of the formation water and an indicator, in most instances qualitative, of pervious/porous horizons and clays.

INDUCTION LOG (DIL), LATEROLOG (DLL)

The induction tool combines an emission coil (current injector) and a receiveing coil (current measuring gauge). The magnetic field created by the emission coil, excited via an oscillator, induces Foucault currents into the formation. Those further generate a magnetic field proportional to the induced current and to formation resistivity accordingly. The double tool (dual induction log-DIL) yields two induction measurements, medium depth and deep respectively. The formation resistivity Rt is derived from a set of type curves. This tool is adequate for insulated drilling fluids (oil base mud, air…) and conductive rocks (clay, marls, silstones, sandstone…) such as those encountered in cover, Molasse type, terrains.

Whenever the formation gets more resistive, as with carbonate, Cretaceous and Jurassic, rocks the dual laterolog (DLL) tool is used (see fig.2 for tool application range). The DLL achieves the penetration of a thin current disk obtained from a barrier (superior and inferior) current forcing the measuring current laterally into the formation. The resistivity of the investigated layer is related to the electrical potential required by the measuring current penetration. Combination of measuring electrodes makes it possible to monitor deep (LLD) and shallow (LLS) currents.

The LLD signal allows a preliminary assessment of formation resitivity Rt. However a precise interpretation requires due correction of borehole, layer thickness and formation invasion effects by means of appropriate type curves.

The current focussing achieved by the DLL tool secures improved vertical resolution, wider resistivity range and better invasion appraisal (Rt / Rm contrast).

DENSITY LOG (LDL)

The tool is based on the principle of density determination utilizing the atom/photon, known also as Gamma/Gamma, interaction. It consists of bombarding the formation from a high energy gamma source and measuring the radiation (re) emittted by Compton effect which prevails, within the concerned energy level (> 1 MeV) over secondary processes such as the photoelectric effect (absorbtion of a photon by an atom and remission of an electron) which occurs at ca 0.1 MeV level, and the production of pairs (electron/positron) at ca 2 MeV.

The electronic density of the (re) emitted radiation is straightforwadly related to actual rock density, in deed a useful property in a sedimentary rock context as the (apparent) electronic density of the rock is very close if not equal to its true density. It appears therefore as a relevant means of identifying lithologies density wise. Interpretation can be enhanced by processing the so called PEF (photo electric factor) via the photoelectric volumetric absorption index (Uma) related to lithology almost independently from porosity (Uma = PEF x ρ).

The tool is also a reliable porosity indicator (which can be correlated with other tools), owing to the density (ρ) porosity (Φ) relationship.

$$\rho = (1-\Phi)\,\rho r + \Phi\rho f \qquad (f = \text{fluid}, r = \text{rock})$$

The LDL (lithodensity log) tool utilises two detectors (as was actually the case for the former FDC tool) equipped with highly sensitive gauges operating within different energy windows enabling to separate the Compton and photoelectric effects.

Density is measured in two detection spaces, long and short respectively, allowing to correct the measurement from the variations of the incident radiation source and borehole/formation environment.

NEUTRON LOG (CNL)

The compensated neutron sonde (CNL) is a nuclear wireline logging tool aimed at a direct porosity measurement, often operated in tandem with the LDL tool.

It utilizes the interaction between a high energy (2 MeV) neutron source and the atomic nuclei of the bombarded formation target. Incident neutrons, after successively colliding (elastic dispersion mode) with nuclei, loose their energy and are, ultimately, absorbed. This neutron capture process can be quantified by measuring the number of collisions needed to lower the energy level to 0.025 eV (thermal level).

This number (nc) is weaker, by one order of magnitude, for hydrogen than for the other elements. As a result the log will be essentially influenced by the number of Hydrogen atoms i.e. by fluids (formation /conate water, liquid/gaseous hydrocarbons) and porosity.

The compensation is designed to minimize the mud noise, by addition of a short sensor, the counting ratio (NPHI) of both long and short signals being less sensitive to mud than both counting processed separately.

However neutron porosity addresses a total and not effective (i.e. that participating to flow) porosity value and needs to be corrected accordingly in particular in argillaceous formations.

SONIC LOG (BHC)

The sonic tool measures the propagation time through the formation of a sonic wave between a source (emitter) and two acoustic receivers. The system is duplicated (in opposing mode) i.e. 1 transmitter, 2 receivers vs 2 receivers, 1 transmitter in order to compensate borehole effects (inclination, excentering, caving, etc…) In a clean formation, sonic porosity Φs is related to log transit time Δt log (µs/ft), by the following equations :

$\Phi s = (\Delta tlog - \Delta tma) / (\Delta tf - \Delta tma)$ Wyllie

$\Phi s = C (\Delta tlog - \Delta tma) / \Delta tlog$ Raymer Hunt Gardner

C # 0.67

Δtma and Δtr are available in tables (ma = matrix, f = fluid)

FORMATION MICROSCANNER (FMS)

The FMS represents the latest development of the (SHDT) dipmeter tool. It releases a formation imaging in terms of electrical conductivities collected via a dense network of sensors (16 microconductivimeters per each sidewall pad) which, in the case of a 4 pad tool, covers up to 40 % of the well openhole sandface ($8"^{1/2}$ drilling diameter). The tool elsewhere includes a sophisticated inclinometer (three component accelerometer and three magnetometers) outfit.

The tool delivers a developped imagery of the well face which is processed according to a fracture oriented rationale (search of fractures, microfissures and rock facies identifiable as dip angles and azimuths).

CEMENT BOND-VARIABLE DENSITY (CBL/VDL)

The casing is vibrated in longitudinal mode via an acoustic source generating compressive (P type) waves. Amplitudes of the acoustic response and transit times are recorded by means of two, one near (3 ft) and one distant (6 ft) , receptors after travelling of the wave train through the casing/cement/formation sequence according to seismic paths dependant on medium acoustic impedances and casing to cement/cement to formation couplings.

The CBL item records the first arrival detected by the near receptor. The VDL item processes later arrivals from the distant receptor and displays through a standard seismic imagery, the (intensity) modulated signal.

Amplitudes and arrival times are processed in order to evaluate the cement to casing and formation bond from their acoustic coupling and typical signatures.

A badly or non cemented casing will undergo resonance, the so called free pipe behaviour. The seismic path will follow the casing and result in short transit times and high amplitudes (strong vibrating energy). Signal amplitude will stand above 10 mV and ultimately reach 50 mV (free pipe threshold).

On the contrary, a good acoustic coupling will show longer arrival times (delayed first arrival), a strong casing signal attenuation and an energetic response from the, behind cement, formation. A bad cement to formation bond would be evidenced by flatening of the amplitude spectrum caused by a week formation coupling and a high attenuation of the signal tail.

These effects can be visualised on the VDL imagery where a free pipe behaviour would be materialised by a set of parallel, black and white, bands as opposed to the herringbone structure characteristic of adequate cement bonding.

The first arrival amplitude is "captured" by an electronic gate, with a very brief opening time, in order to record maximum signal amplitude. This process may be affected by two artifacts, induced on travel time monitoring by low signal amplitudes thus indicative, in most cases, of a good cement bond, stretching and cycle skipping respectively.

Cementing performance can be biased by channeling and microannulus effects. Channeling consits of fluid flow paths filled with mud, water, gas or/and drilling completion fluids, within the cement mass. A microannulus is a consequence of the presence, between the casing and the cement, of a thin, pellicular, fluid film.

The CBL/VDL is sensitive to microannulus where as channeling noise is better appraised by the USI tool.

ULTRASONIC INSPECTION TOOL (USIT)

The USIT which combines both cement evaluation and corrosion control functions prolonges and progressively replaces the former CET and BHTV tools.

It allows to vibrate the casing in both longitudinal (P waves) and transverse (S waves) modes via a rotating ultrasonic source generating pulsed trains of compressional and shear waves and to process, radially, arrival times and amplitudes.

Its resolution capacity - 72 radial measurements, vertical space increment of 0.5"- places it as a sophisticated, though sometimes ambiguous as to log interpretation, inspection logging tool.

Log outputs address essentially casing inside diameters (processing of first arrival times), thickness and filling of casing to formation or casing to casing annulus i.e. cement evalutation. The latter feature eases the detection of channeling effects.

BOREHOLE GEOMETRY (BGL)

It includes a four arm caliper whose deflections are processed vis-à-vis, thus delivering two mean diameter values.

It can be assisted by an inclinometer telemetry, useful in correlating well geometry to trajectory changes in a cursory manner however as compared to thorough directional surveys. It displays, alongside borehole diameters, annular volumes indicative of hole caving and further cementing volume requirements.

PRODUCTION LOGGING TOOLS (PLT)

Those consist of temperature and pressure sensors, openhole flowmetering spinners and, occasionally, openhole calipers operated either separately, by pairs or all together in a thorough combined production logging tool.

Measuring principles :

- *Temperature*. Platin thermistor
- *Pressure*. Strain gauge, Bourdon type gauges, quartz piezoelectric gauges (vibrating frequency proportional to the pressure applied to crystal faces) continuously temperature compensated, piezoresistive gauges. Whenever no multiple nor monoconductor cables are available, a simplified slick line and quartz memory gauge outfit is utilised instead. The latter has replaced the former, now obsolete, downhole Amerada/Custer gauges.
- *Flowmetering*. Borehole micro spinners are utilised to monitor, preferably counter current wise, fluid ascending speeds. Whenever low to very flow conditions prevail a so called petal like full bore high resolution tool is recommended.

A conventional openhole three arm caliper is often required to correct speeds from borehole irregularities (caving) and release true flowrates accordingly.

The flowmeter tool is most relevant in indentifying reservoir productive intervals, interlayer crossflow and related thief zones.

CASING CALIPERS

Casing inspection, in the sense of inside diameters (IDs), is performed via multifinger caliper tools, namely.

- *Tubing geometry sonde (TGS)*. The 16 arm caliper limitation in circumferencial resolution (ca 22 °/arm) is compensated by (i) the simultaneous recording of 16 radius (8 diameter) measurements, and (ii) an excentralising correction, assuming a circular (non ovalised) casing geometry, useful in highly deviated wells. The tool is available for up to 7" casings.
- *40 to 72 multifinger (casing inspection calipers - CIC)*. The most commonly used tool is a 40 or 60 arm device delivering two, one minimum and one maximum, casing IDs.
- *72 arm zonal apparatus (multifinger caliper tool MFCT)* recording over 36 areas (each 10° in coverage) minimum, maximum and mean IDs for 9"$^{5/8}$ to 13"$^{3/8}$ casings.

A sophisticated 40 arm caliper, available for 7" and 9"$^{5/8}$ casings, achieves the simultaneous recording of 40 radii (20 IDs).

Such tools are extensively utilised to investigate casing status, assess wall roughness and evidence corrosion/scaling damage.

4. WELL TESTING PRINCIPLES

- **The diffusivity equation**

Horizontal, single phase, flow in a homogeneous, isotropic, non compressible porous medium of constant thickness and infinite radial extent is expressed, further assuming negligible gravity and thermal effects, by the diffusivity equation (see nomenclature in table 3) :

(1) $$\frac{\partial^2 p}{\partial r^2}+\frac{1}{r}\frac{\partial p}{\partial r}=\frac{\phi\mu c_t}{k}\frac{\partial p}{\partial t}$$

whose solution, subject to the following initial and boundary conditions

(2) $p(r,o) = pi$ for any r

$p(\infty,t) = pi$ $t > o$

$$\lim_{r\to 0}\left(r\frac{\partial p}{\partial r}\right)=\frac{q\mu}{2\pi kh}$$

is expressed as :

(3) $$p_i - p = \frac{q\mu}{2\pi kh}\left[-Ei(u)\right]$$

with : Ei(u) = exponential integral function

$u = \phi\mu c_t r^2/4\,kt$

For small values of u say $u<10^{-2}$ (3) reduces to the semi logarithmic approximation :

(4) $$p_i - p = 0.183\frac{q\mu}{kh}\left[\log\left(\frac{kt}{\phi\mu c_t r^2}\right)+0.351\right]$$

(3) and (4) set the bases for the analysis and interpretation of well test pressure transients.

Solution (3) is exploited by superposition of the bottomhole pressures vs time log-log plot to the –Ei(-u) type curve (identification or match-point method)

Solution (4) enables to derive the straight line slope (m) of the semi-log plot of presssures vs times (semli-log analysis).

- **Solution gases**

Although the formation fluid is assumed single phase liquid (water) it contains, in most instances, a dissolved gaseous phase quantified by PVT analysis in terms of gas water ratio, and bubble point, dew point pressures. Therefore a coefficient, known as the volume factor B, expressed as the ratio of the water and solution gas volume (under reservoir conditions) to the water volume (at standard conditions) is applied to correct flowrates q. In most low enthalpy geothermal well tests B = 1.

- **Wellbore and sandface effects**
  - *Wellbore storage*

It results from either fluid expansion or changing liquid levels within the well. It is expressed for a produced liquid volume V under a pressure drop Δp as :

(5) $C = V/\Delta p$

Wellbore storage occurs during the early times of well testing and is of limited, if not negligible, impact on wells exhibiting high deliverabilities. Note that it can be offset by measuring the sandface flowrate downhole.

- *Skin effect*

Skin is cause by local heterogeneities of reservoir permeability at and close to the sandface. This pellicular effect can be a consequence of a mud cake and/or filtrate invasion in which case the local permeability decreases (positive skin, damaged well). Conversely, well stimulation would locally upgrade reservoir permeability (negative skin, stimulated well).

The magnitude of the skin induced pressure Δps is appraised through the skin factor

(6) $$S = \frac{2\pi kh}{qB\mu}\Delta ps$$

- **Well test interpretation**

Whenever an observation well at a distance r of the producing well (case of an interference test) is not available, pressures are monitored and processed on the sole producing well and r will be set equal to well radius r_w in compliance with the line source approximation adopted in the sandface flow boundary condition (2). In the forthcoming p will referred to as the well flowing pressure p_{wf} (see table 3).

- *Log-log plot. Type curve/match point analysis*

The reservoir is assumed of infinite radial extent and the well subjected neither to wellbore storage nor skin effect.

Using the reduced variables, listed in table 3, the pressure transient response will conform to :

(7) $$p_D = \frac{1}{2}E_i\left(-r_D^2/4t_D\right)$$

The interpretation exercise consists of superposing the pressure vs time log-log plot to type curve (7) until achieving the best possible fit and deriving reservoir permeability k (or transmissity kh) and total compressibility c_t or porosity ϕ from match point coordinates (in consistent units, table 3) :

(8) $$\log\Delta p = \log p_D - \log\frac{2\pi kh}{qB\mu}$$

(9) $$\log t = \log t_D - \log\frac{kt}{\phi\mu c_t r^2}$$

The example shown in fig. 3 addresses a set of type curves including the additionnal dimensionless wellbore storage coefficient C_D and skin factor S, which actually may render the interpretation somewhat ambiguous regarding uniqueness of the solution.

- *Semi-log plot straight line analysis*

It is a less straight forward analysis than the previous log-log approach bearing in mind that the straight line behaviour is expected to start after an elapsed time of ca two hours owing to the validity range of the semi-log approximation and to wellbore storage effects.

Regardless of wellbore storage, which can be estimated independantly (see ref. 5) and is elsewhere of moderate interest regarding reservoir analysis, the straight line slope, illustrated in fig.3, allows to determine both permeability and skin from the following equations.

(10) $m = 0.183\, qB\mu / kh$

(11) $$S = 1.151\left[\frac{p_i - p_{1hr}}{m} - \log\left(\frac{k}{\phi\mu c_t r_w^2}\right) + 3.23\right]$$

- **Boundary effects**
  - *Closed reservoir*

As opposed to the infinite acting reservoir, whose pressure stabilises at some distance of the well (fig. 4a), a closed reservoir would display pressure profiles indicative of a uniform depletion rate. The latter, illustrated in fig. 4b is referred to as pseudosteady state, which can be misleading as the system never reaches stabilization.

Pressure decline of a closed boundary reservoir follows a straight line trend in cartesian coordinates which deserves a cautious analysis, a matter discussed in ref. 5.

- *Impervious boundaries*

A no flow boundary, of the fault type assumed linear in shape, leads to a doubling of the straight line slope in the semi logarithmic representation described in fig. 5a.

- *Recharge boundaries*

Similarily, a constant pressure boundary would act as a recharge line achieving steady state according to the straight line departure and pressure stabilisation trends exemplified in fig. 5b.

- **Superposition principle**

The linearity of the diffusivity equation allows to superpose the pressure transient responses respective to space and time.

- *Boundary equivalences. Images*

Two wells discharging at identical rates generate a zero flow line at mid well spacing.

Consequently this symetry allows to replace the system by a single well/impervious boundary "mirror" representation. Vice-versa an impermeable barrier can be reciprocated via an image well discharging at the same rate at a two fold well to barrier distance.

Conversely a recharge boundary would be represented by a two well system with an image injection well (-q recharge).

As a matter of fact the latter reflects the popular well doublet concept of heat mining, combining a producer and an injector well at a distance d, widely applied in geothermal district heating. As a result of the superposition principle the flowing pressure drop at the discharging well will be expressed as :

$$(12) \quad p_i - p_{wf} = \frac{qB\mu}{kh}\log\left(\frac{d}{r_w}\right) + 0.44\frac{qB\mu}{kh}S$$

which is no longer time dependant.

A more general illustration of the image method is systematised in the rectangular shaped closed system depicted in fig. 6.

- *Multirate tests*

The effect of wells can be added at different times. This applies to several wells exhibiting different production/injection sequances and, likewise, to a single well discharging at variable ratse. In this case it is advised to substitute to the standard (pi - p_{wf}) vs logt plot a, rate normalised,

$$\left(p_i - p_{wf}\right)/q_N \quad vs \quad \sum_{I}^{N}\left[\frac{q_i - q_{i-1}}{q_N}\log\left(t - t_{i-1}\right)\right] \quad plot$$

- **Pressure buildup**

Previous sections addressed the pressure drawdown stages of well tests.

The superposition principle can be extended to the processing of the pressure recovery stage further to well shut in. This is achieved by adding the pressure responses to production rate + q prolonged over the actual production duration tp (i.e. time $t_p + \Delta t$) and to an injection rate –q strating at t_p (i.e. time Δt), thus leading to :

$$(13) \quad p_i - p_{ws} = \Delta p\,(+q, t_p + \Delta t) + \Delta p\,(-q, \Delta t)$$

(14) $$p_i - p_{ws} = \frac{0.183Bq\mu}{kh}\left[\log\frac{k(t_p+\Delta t)}{\phi\mu c_t r_w^2} - \log\frac{k\Delta t}{\phi\mu c_t r_w^{é}}\right]$$

(15) $$p_i - p_{ws} = \frac{0.183Bq\mu}{kh}\left[\log\frac{t_p+\Delta t}{\Delta t}\right]$$

As a result the semi-log straight line analysis can be applied to the pressure buildup by plotting pressures p_{ws} (measured from p_{wf} (t_p)) against (t_p + Δt)/ Δt known as the Horner plot.

In addition to the kh product, pressure buildup analysis delivers the skin factor by substitution of th Δt = 1hr pressure :

(16) $$S = 1.151\left[\frac{p_{1hr} - p_{wf}}{m} - \log\frac{kt_p}{(1+t_p)\phi\mu c_t r_w^2} + 3.23\right]$$

The initial reservoir pressure p_i may also be derived by extrapolating to 1 (infinite Δt) the straight line fraction of the Horner plot.

- **Fractured wells and reservoirs**

Hydraulic fracturing is a routine technique in stimulating wells. Hydraulic fracturing will create, owing to the state of in situ stresses prevailing at depth, a vertical fracture of lenght x_f assumed to penetrate the whole produced formation as shown in fig. 7.

- *Finite conductivity fractures*

The three drainage mechanismes, bilinear, linear and radial flow respectively, are described in fig. 8.

Bilinear flow, combining linear flows from the fracture and surrounding formation, occurs at early times and exhibits a straight line behaviour with a 1/4 slope on the log-log plot shown in fig. 9, according to the following equation :

(17) $$p_D = \frac{2.451}{\sqrt{k_{fD} w_{fD}}} t_D^{1/4} x_f$$

with :

(18) $k_{fD} = k_f/k$ reduced fracture permeability

$w_{fD} = w/x_f$ reduced fracture width

With increasing times the flow regime moves towards linear flow recognisable on fig. 9 as a ½ slope linear trend.

This transitional phase is often masked by the ultimate radial flow pattern

- *. Infinite conductivity fractures*

This configuration applies whenever the k_{fD} product is larger than 300. In such a case there is no bilinear flow and linear flow prevails instead, with reduced pressure conforming to :

(19) $$p_D = (\pi t_{Dxf})^{1/2}$$

i.e. a ½ slope on a Δp vs time log-log plot

- **Dual porosity**

Many reservoirs produce from naturally fractured formations combining high permeabilities from the, socalled, secondary porosity, represented by the fractured space, and lower porosities and permeability of the rock matrix environment.

The approach pioneered by Warren and Root (ref.4) assumes that the actual fractured reservoir can be modelled by the orthogonal matrix blocks and adjacent fractures system depicted in fig.10.

Worth mentioning also are the horizontally stratified sedimentary sequences including alternating pervious (secondary porosity) and semi pervious (primary porosity) layers which often exhibit a double porosity behaviour.

Two parameters are used to formalise the pressure transient responses of a dual porosity system, fluid storativity in both rock matrix (primary porosity) and fractures (secondary porosity) and transmissivity of fractures respectively (ref.5 and 7). In other terms, fluid filled fractures intersected by the well are assumed to further drain the connected matrix and feed the producing well . Hence well pressures respond first to fracture flow taking into account fracture conductivity (or transmissivity) and storage. The matrix secondary response is significantly delayed thus giving rise to the two straight line signature evidenced in fig.11a and b semilog plots.

The interpretation leans on the variables and parameters defined here after (ref.5)

- reduced variables

(20)
$$p_D = \frac{k_f h}{0.183 q B \mu} \Delta p$$
$$t_D = \frac{k_f t}{(\Phi_f c_{tf} + \Phi_m c_m)\mu r_w^2}$$

- parameters

(21)
$$\omega = \Phi_f c_{tf} / (\Phi_f c_{tf} + \Phi_m c_m) \qquad storativity\ ratio$$
$$\lambda = \alpha \frac{k_m}{k_f} r_w^2 \qquad transmissivity\ ratio$$

with :

(22)
$$\alpha = \begin{cases} 60 / x_m^2 & \text{cube shaped blocks of size } x_m \\ 12 / h_f^2 & \text{horizontally stratified parallelipedic slabs of hf fracture thickness} \end{cases}$$

If ω=1 and $\lambda > 10^{-3}$ double porosity reduces to a single porosity behaviour.

- **Pressure derivative**

The time pressure derivative concept, first perceived by Shell oil by which placed a patent on the topic, has raised considerable interest since the works of Bourdet et al (ref.5) and the advent of modern pressure recording devices (quartz gauges) substituted to the former, now obsolete, Amerada/Custer bomb technology, and subsequent computer processing and graphic displays.

It has become nowadays a standard in well test interpretation.

The derivative plot, of the type illustrated in fig. 12, displays, on a log-log scale, two simultaneous Δp vs Δt and tdp/dt vs Δt curves.

The salient feature of this presentation lies on that it concentrates on a single graph the information on many well and reservoir parameters, through typical pressure derivative signatures, for instance (see fig. 13)

- infinite acting reservoir : flat section
- closed reservoir (pseudo steady state : steep rising straight line of unit slope)
- impervious boundary :second flat section at late times
- constant pressure boundary : constantly decreasing line
- dual porosity behaviour : presence of a minimum for late times

The extension to pressure buildups is somewhat more delicate and interpretative ambiguities lifted in the case of the infinite acting reservoir setting.

- **Interference tests**

Such tests, asssociating a multiwell array, including at least one (shut in) observation well, provide invaluable clues on formation characteristics to reservoir engineers thus widening the scope of single well pressure drawdown/buildup analysis alone. They are of particular relevance to reservoir simulation and related model calibration, history matching, stages.

Interference tests address much larger reservoir areas therefore strenghtening the averaging effect mentioned previously for single well tests analysis. They are most useful in determining preferential flow paths, identifying lateral boundary behaviours, field singularities and anisotropy patterns not obtained from standard well test. Last but not least they enable to reliably estimate reservoir porosities.

Interpretation of interference tests is based on the flow superposition principle developed earlier.

Special care is to be brought in test design and programming production well shut in sequences accordingly. Simulation codes are recommanded while processing pressure transients in order to achieve pertinent interpretation.

- **Miscellaneous tests**
  - *Injection tests*

Pressure rise and fall off tests replicate the pressure drawdown and buildup tests analysed previously. However injection testing must account for temperature induced effects and related mobility changes.

  - *Drill stem tests (DST)*

DSTs are useful aids in accessing reservoir performance during drilling. The testing outfit includes a drill string connected to downhole, either single or straddle, packer and (surface actuated) valve assembly. The test is conducted according to a double shut in sequence. The well is first flowed over a short period to secure equalising with reservoir pressure then shut in to estimate reservoir static pressure . The second, longer lasting, flowing and shut in periods give access to standard drawdown and buildup analysis. Flowrates, which are time varying, are measured from either drillpipe filling (non flowing well) or from surface free flows (self flowing well). In non flowing wells monitoring of rising water levels during the final recovery stage may upgrade the buildup analysis.

  - *Step drawdown tests*

They aim at producing the well delivery (stabilised pressures against of is change rates) curve, assessing nominal well productive capacity and designing submersible pump characteristics.

On a geothermal well doublet, stabilised pressure (Δp_{wh}) at production well head is often expressed as follows (in practical units and assuming B=1)

(a) $\Delta p_{wh} = \Delta p_d + \Delta p_s + \Delta p_c$

(b) $\Delta p_d = \frac{q\mu}{kh} \log\left(\frac{d}{r_w}\right)$ dynamic (flowing) pressure drop

(d = top reservoir well spacing)

(23) (c) $\Delta p_s = 0.44 \frac{q\mu}{kh} S$ skin pressure change

(S skin factor)

(d) $\Delta p_c = 1.610^{-12} \frac{\mu^{0.21} q^{1.79} l_c}{r_c^{4.79}}$ casing friction losses

(r_c, l_c casing radius and length)

units : Δp (bars) ; q (m^3/hr) ; kd (dm) ; μ(cp) ;
d, r_w, r_c, l_c, (m)

For the injection well a thermosiphon pressure drop Δp_{ts} is added :

(24) $\Delta p_{ts} = 9.8110^{-5} [\rho_o - \rho_i] z$

$\rho_o - \rho_i$ = formation and injected fluid densities (kg/m^3)
z = vertical reservoir depth (m)

- **Well testing summary**

Graphic displays, by means of Δp and tdp/dt vs time log-log and semi-log plots, form the basis of well test analysis and identification of the reservoir parameters and flow mechanismes involded.

The foregoing are summarised in table 4 which provides a thorough review of the graphical signatures and plots utilised respective to the concerned flow mechanisms.

This review is complemented by fig. 14 semi-log and log-log synthetic representations which allow to visualise, from early to late elapsed times, wellbore, transient, infinite acting radial flow and boundary effects.

FIELD APPLICATIONS

- **Exploration well logging**

Fig. 15 and 16 illustrate log outputs selected on a geothermal wildcat (see logging programme in table 5).

Fig. 15 is a composite production log combining an openhole 3 arm caliper, temperature and (full bore petal like) flowmeter tools on the target reservoir interval. Note the correlations between borehole caving and temperature convection on the 2100 and 2200 m depth interval. Fluid velocities need to be corrected from caving effects but indicate howewer a significant flow contribution from the afore mentioned interval.

Fig. 16 displays a fracture evaluation exercised by processing of FMS imagery in the sense of fracture and dip intensities (stereonets) and fracture aperture vs depths and azimuths.

- **Development well logging**

The composite well log represented in fig. 17 concentrates a dense information, over the bottomhole geothermal reservoir, issued by caliper, GR, BHC, LDL, temperature and flowmeter tools. This document shows actually good agreement between the porosity (from sonic and density) peaks above the 15 % (LDL) and 12 % (BHC) cut off values and the producing (pay) zone evidenced by flowmetering (expressed as percentages of total cumulated flowrate). The temperature log appears here as a gross indicator of the whole reservoir (total pay) traced through the strong convection hump and related temperature reversal noticed on the 1925 to 2005 m depth interval. This thick (80 m) zone was further well tested exhibiting a prolific yield (300 m^3/hr self flowing capacity) and dependable characteristics (kh = 90 dm and S = -1.5). The whole logging programme is listed in table 6.

- **Exploitation well inspection**

Fig. 18 shows a variety of damaged (and restored) casing states appraised by multifinger calipers. Fig. 18 displays typical signatures of non damaged and damaged (corrosion/scaling episodes) casings achieved by conventional 40 arm inspection tools delivering a minimum and a maximum ID. Fig.18b desmonstrates the ability of a 40, simultaneously recording, finger caliper ins assessing casing roughness and wall upgrading further to jetting clean up. Fig. 18c gives thickness and radial image of casing damage and ultimate piercing provided by the 16 (simultaneously recording) finger (TGS) tool.

Logging and testing programmes are presented in table 7.

- **Well testing. Pressure drawdown analysis**

Fig. 19 is a computer assisted test processing and interpretation of pressure buildup sequences.

The MDH semi-log plot (fig. 19b) delivers as usually in such short (several hours) testing periods an overestimated kh value (59 000 mdm) compared to the more realistic figure (45000 mdm) derived from the Horner plot (fig. 19c).

Note the flatening of the late time pressure derivative plot indicative of an infinite acting reservoir.

- **Interference and injectivity testing**

Fig. 20 summarises a long lasting field testing programme carried out on a well doublet in order to assess the injective performance of a deep seated sandstone reservoir.

Testing consisted of interference (producing/injecting well 1, observation well 2 and vice versa), injectivity and loop circulation tests and of the field outfit (fluid pumping/storage/treatment/monitoring facilities and downhole pressure/temperature gauges) sketched in fig. 20a.

Test interpretation leaned on pressure buildup and falloff analysis prior to and after well acidising.

Ultimate test results exemplified on the fig. 20b cartesian plot led to the following diagnosis with respect to well and reservoir injective capacities.

On well 1 pressure reaches stabilisation. However surface injection pressure remains high. This behaviours is symptomatic of a (removable) damage of mechanical origin, caused by an odd completion (gravel pack placement) and the displacement in the annular space of large size particle aggregates which bridge the well sandface. Damage may be removed by backwashing.

Well 2 reflects a typical formation invasion process by fine, non filtered, particles. In such a case pressure does not stabilise because of formation plugging and likely erosion due to high injection velocities at sandface mainly.

.

TABLE 1: BASIC FORMULAE USED IN LOG INTERPRETATION (after Schlumberger)

(1) $SP = - K \log (Rmf/Rw)$

2) $F = Ro/Rw = a / \Phi^2$

(2') a=1 *Archie*
(2") a = 0.81 *Humble*

(3) $Sw = (Ro/Rt)^{1/2}$

(4) $(Sw/Sxo) = \left(\frac{Rxo/Rt}{Rmf/Rw} \right)^{1/2}$

(5) $ts = \Phi t_f + (1- \Phi) t_{ma}$

(6) $\Phi = (T_s – T_{ma}) / (T_f – T_{ma})$ *Wyllie*

(6') $\Phi = 0.67 (T_s – T_{ma}) / T$ *Raymer-Hunt-Gardner*

(7) $pb = \Phi p_f + (1-\Phi) p_{ma}$

(8) $\Phi = (p_{ma} - p_b) / (p_{ma} - p_f)$

Parameters

F = formation factor
K = SP (temperature dependant) constant
R = resistivity
S = saturation index
SP = Spontaneous (self) potential
T = transit time
p = density
Φ = porosity

Subscripts

b = bulk rock
f = fluid
ma = matrix
mc = mud cake
mf = mud filtrate
o = (clear water saturated formation)
t = clean formation
s = sonic
w = water
xo = flushed zone

TABLE 2: BASIC LOGGING TOOL NOMENCLATURE

LOG NAME	ABBREVATION	WELL STATUS	APPLICATION
Gamma Ray	GR	OH, CH	Argillosity Lithology marker
Spontaneous (Self) potential	SP	OH	Lithology, porous/pervious layer marker
Dual Induction	DIL	OH	Lithology, formation resistivity
Dual Laterolog	DLL	OH	Lithology, formation resistivity
Litho Density	LDL	OH	Lithology, density, porosity Porosity/lithology crossplots
Compensated neutron	CNL	OH, CH	Porosity. Porosity/lithology crossplots
Borehole Compensated Sonic	BHC	OH	Porosity. Porosity/lithology crossplots
Formation Micro Scanner	FMC	OH	Extension of the dipmeter tool (SHDT). Formation imagery. Fracture processing
Borehole Geometry, Caliper	BGL, CAL	OH	OH diameter, annular cement volumes
Cement Bond, Variable Density	CBL/VDL	CH	Cementing control
Ultrasonic Inspection	USIT	CH	Cementing control Inside casing inspection
High Resolution Thermometery	HRT	OH, CH	Dynamic/static temperature profile
Quartz Pressure gauge	QPG	OH, CH	Dynamic/static pressure profile
Production Logging	PLT, PCT	OH	Combined (pressure, temperature, flow) tool.
Full Bore Spinner flowmeter		CH	Low speed well flowmetering (petal device)
Continuous Flowmeter		OH, CH	Flow profile
Tubing Geometry Sonde	TGS	CH	Casing ID, 16 arm, simultaneously recorded deflections
Multifinger Casing Caliper	MFCL	CH	40 to 60 arm tool Max/Min casing ID
Casing Inspection Caliper	CIC	CH	40 to 60 arm tool Max/Min casing ID
Fluid Sampler	FS	OH, CH	Bottom hole sampling (PVT analysis)

CH = Cased hole
OH = Open hole

TABLE 3: VARIABLES, EQUATIONS AND UNITS USED IN WELL TESTING

Symbol	Definition	Oilfield units	Metric units
P	Pressure	psi	bar
P_i	Initial reservoir pressure	psi	bar
P_{wf}	Well flowing pressure	psi	bar
ΔP_s	Skin induced pressure change	psi	bar
q	Production (injection) rate	STB/d	m^3/hr
r	Radial distance	ft	m
r_w	Wellbore radius	ft	m
t	Time	hr	hr
B	Formation volume factor	(res vol/std vol)	(res vol/std vol)
C	Wellbore storage coefficient	STB /psi	STm^3/bar
k	Intrinsic permeability	md	d
h	Reservoir net thickness	ft	m
c_t	Total compressibility factor	psi^{-1}	bar^{-1}
ϕ	Porosity		
μ	Dynamic viscosity	cp	cp
P_d	Reduced pressure	$\frac{kh\,(p_i-p_{wf})}{141.2\,qB\mu}$	$\frac{2\pi\,kh\,(p_i-p_{wf})}{qB\mu}$
t_D	Reduced time	$\frac{0.000264\,kt}{\phi\mu c_t r_w^2}$	$\frac{kt\quad.}{\phi\mu c_t r_w^2}$
r_d	Reduced radius	r/rw	r/rw
C_d	Dimensionless wellbore storage	$\frac{5.615\,C}{2\pi\phi\,c_t\,hr_w^2}$	$\frac{C\quad.}{2\pi\phi\,c_t\,hr_w^2}$
m	Slope straight line semi-log plot	$\frac{162.6\,qB\mu}{kh}$	$\frac{0.183\,qB\mu}{kh}$
S	Skin factor	$\frac{kh}{191.2qB\mu}\Delta p_S$	$\frac{2\pi kh}{qB\mu}\Delta p_S$

TABLE 4: WELL TESTING GRAPHICAL DISPLAYS (SOURCE R.N. HORNE REF. 5)

Flow mechanism	Characteristic	Plot
Infinite-acting radial flow (drawdown)	Semilog straight line	p vs. log Δt, (semilog plot, sometimes called MDH plot)
Infinite-acting radial flow (buildup)	Horner straight line	p vs. log $\Delta(t_p+\Delta t)/\Delta t$, (Horner plot)
Wellbore storage	Straight line p vs. t, or Unit slope log Δp vs. log Δt	log Δp vs. log Δt, (log-log plot, type curve)
Finite conductivity fracture	Straight line slope ¼, log Δp vs. log Δt plot	log Δp vs. log Δt, or Δp vs. $\Delta t^{1/4}$
Infinite conductivity fracture	Straight line slope ½, log Δp vs. log Δt plot	log Δp vs. log Δt, or Δp vs. $\Delta t^{1/2}$
Dual porosity behavior	S-shaped transition between parallel semilog straight lines	p vs. log Δt, (semilog plot)
Closed boundary	Pseudosteady state, pressure linear with time	p vs. Δt, (Cartesian plot *)
Impermeable fault	Doubling of slope on semilog straight line	p vs. log Δt, (semilog plot)
Constant pressure boundary	Constant pressure, flat line on all p,t plots	Any

(*) Not recommended

TABLE 5: EXPLORATORY WELL LOGGING PROGRAMME

TOOL	DEPTH INTERVAL m	WELL/LOG STATUS	REMARKS
BGL	0 – 2680	OH	Cement volume
BGL/GR		OH	OH flow section
DIL/SP/GR	0-1370	OH	Upper clastics Lithology, porosity
DLL/GR	1375 – 2680	OH	Lower carbonate lithology
BHC/GR	1375 – 2680	OH	Porosity
FMS/GR	1790 – 2680	OH	Reservoir fracturing
LDL/CNL/GR	1375 – 2680	OH	Neutron/density porosities
HRT	0 – 2680	OH/CH	Static/dynamic temperature profile
QPG	0 –2680	OH/PRO	Static/dynamic profile
PLT	1375 – 2680	OH/PRO	Full bore tool
QPG	2500	OH/PRO	Pressure buildup
BHS	2600	OH/PRO	PVT
GR/CCL	1790 - 2680	OH/CH	

OH Openhole
CH Cased hole
PRO Production logging

TABLE 6: DEVELOPMENT WELL LOGGING PROGRAMME

TOOL	DEPTH INTERVAL (m)	WELL/LOG STATUS	REMARKS
BGL/GR	359 – 1905	OH	Cement volume
CBL/VDL/GR	338 – 1880	CH	Cement control
LDR/GR	1907 – 2109	OH	Reservoir only. Lithology / porosity
BGT/BHC/GR	1907 – 2109	OH	Reservoir only. Porosity and diameter
MFCT	+2 – 1895	CH	Inside casing status
USIT	10 – 1906	CH	Corrosion / cement control
PLT	1907 – 2083	OH/PRO	Producing intervals
QPG	1911	OH/PRO	Pressure draw down / build up
BHS	2060	OH/PRO	PVT

TABLE 7: OPERATING PRODUCTION / INJECTION WELLS
TYPICAL INSPECTION LOGGING / TESTING PROGRAMMES

TOOL	APPLICATIONS
MFCT/CIC	Casing integrity control (as of IDs) and roughness analysis
CCL	Well total depth control via sinker bars and cable tension recording
CBL/VDL/GR	Standard cementing control
USIT	Additional casing integrity and cementing control
RBP	Casing pressurizing tests via packer (two single or straddle packer string) leak off tests
BGT/GR	Openhole diameter control
QPG	Well testing, single production or injection wells Combined production / injection well (loop) testing Interference test
PLT	Combined flowmeter and temperature analysis for casing leak detection or matching of openhole producing/ injecting levels
FS	PVT sampling

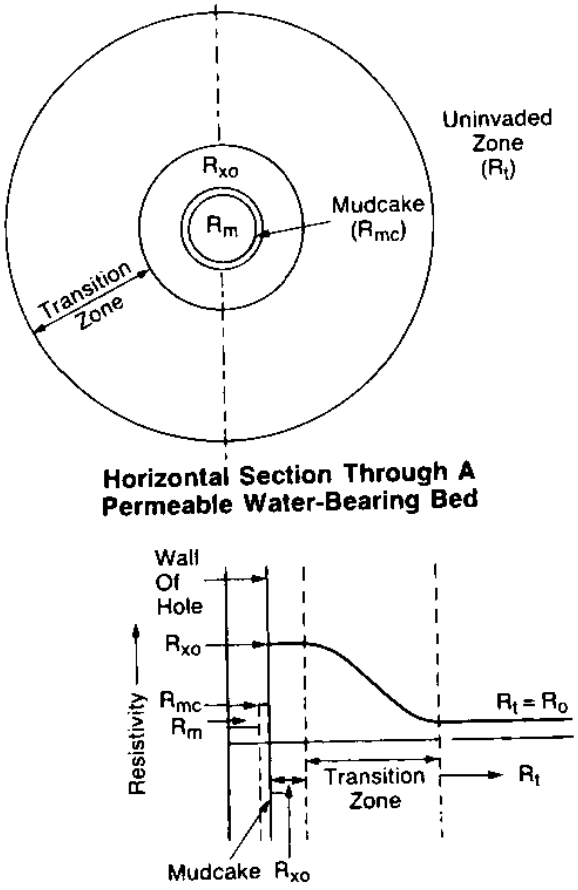

Figure 1: Radial distribution of resistivities (R_{mf}>>R_w, Water – Bearing Bed) (source: Schlumberger ref. 1)

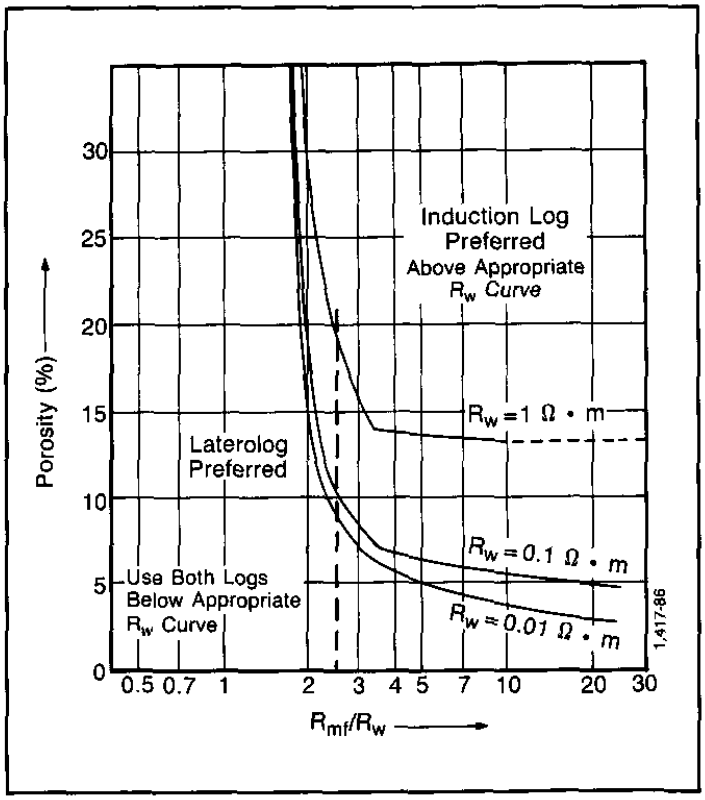

Figure 2: Preferred ranges of application of induction logs and laterologs (source: Schlumberger, ref. 1)

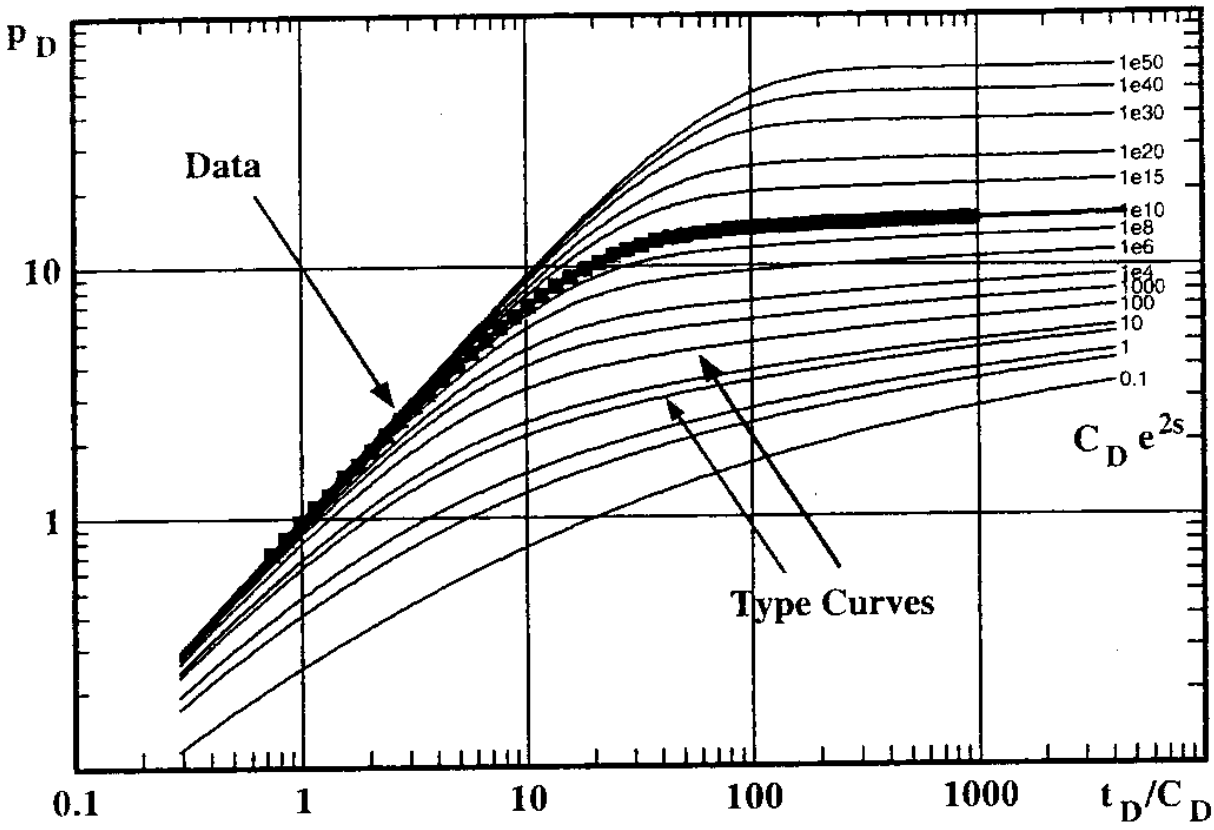

Figure 3: Log – Log plot – Type curve method (source R.N. Horne ref. 5)

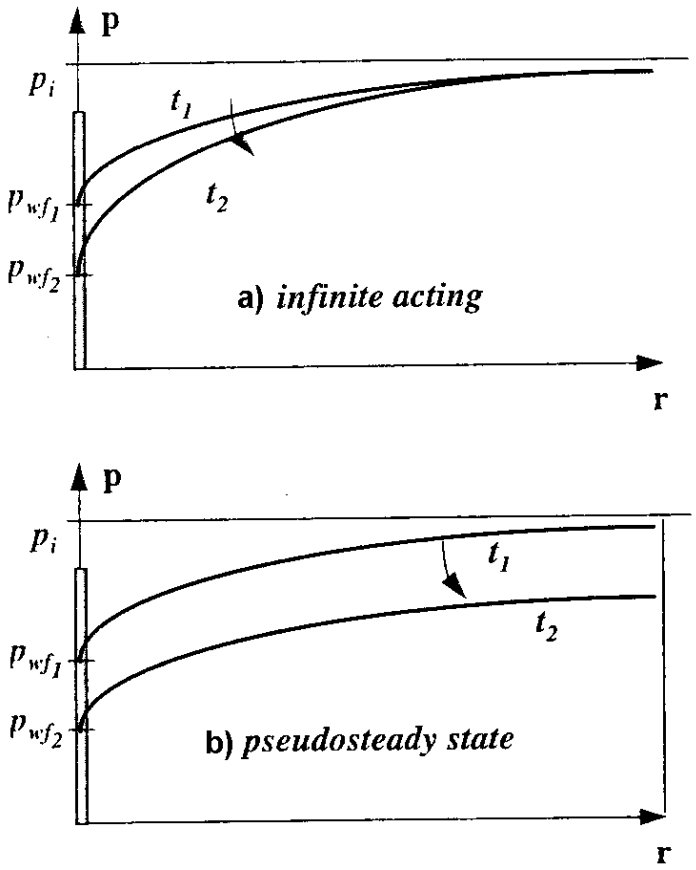

Figure 4: Semi – log plot – Boundary effects

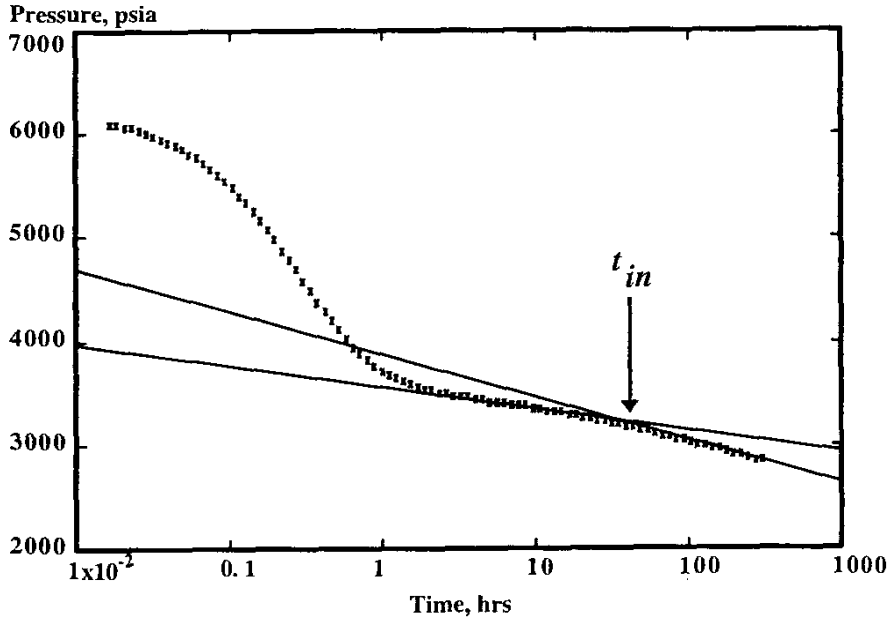

Figure 5a: Impervious boundary

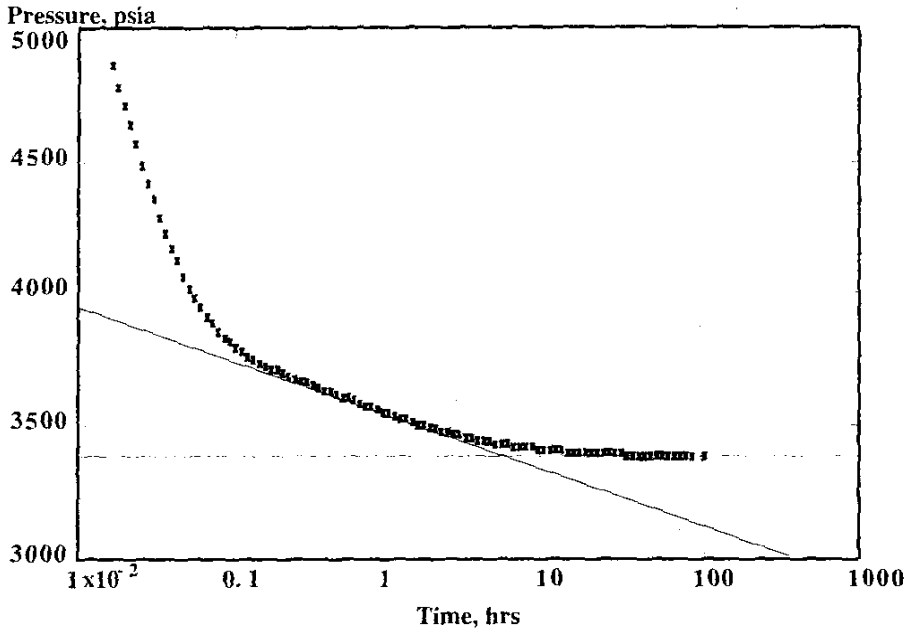

Figure 5b: Recharge boundary

Figure 5: Semi – Log Plot – Boundary effects (source R.N. Horne, ref. 5)

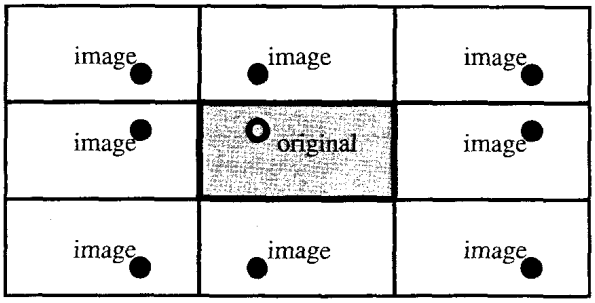

Figure 6: Closed reservoir – Image method (source R.N. Horne, ref. 5)

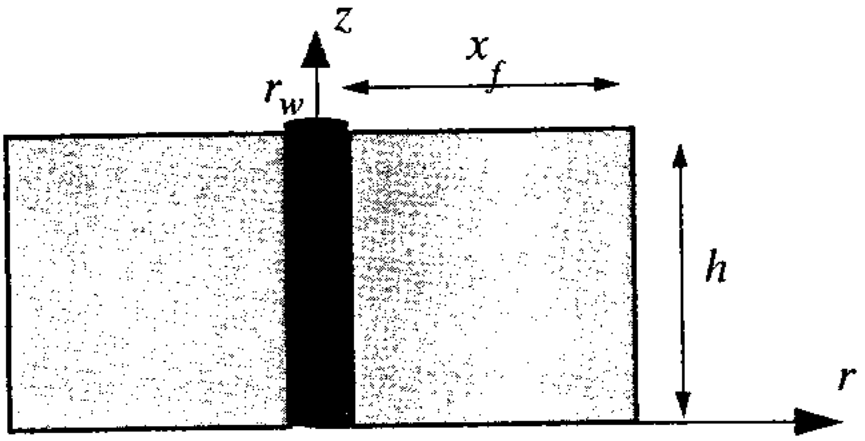

Figure 7: Fully penetrating finite fracture (source R.N. Horne, ref. 5)

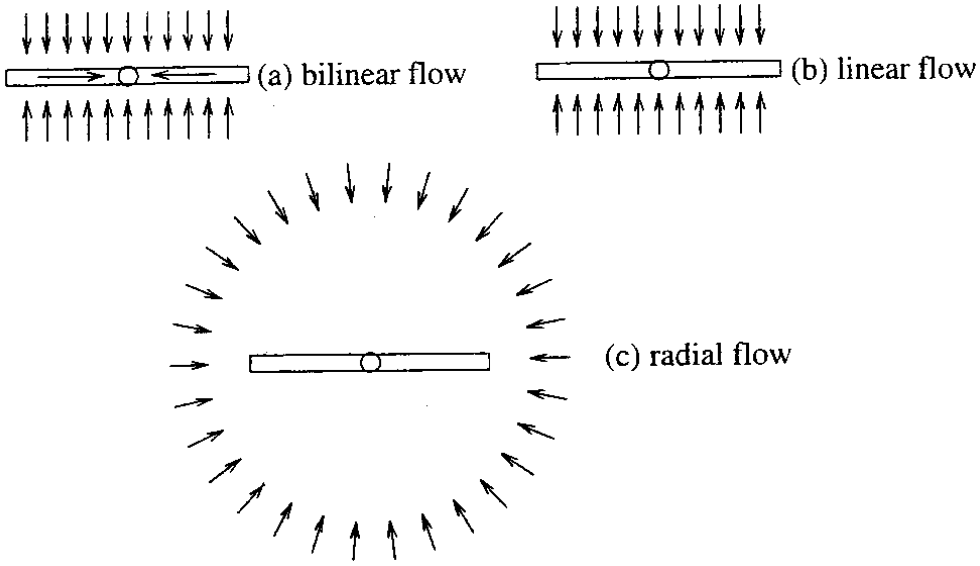

Figure 8: Flow regimes – Finite fracture (source R.N. Horne, ref. 5)

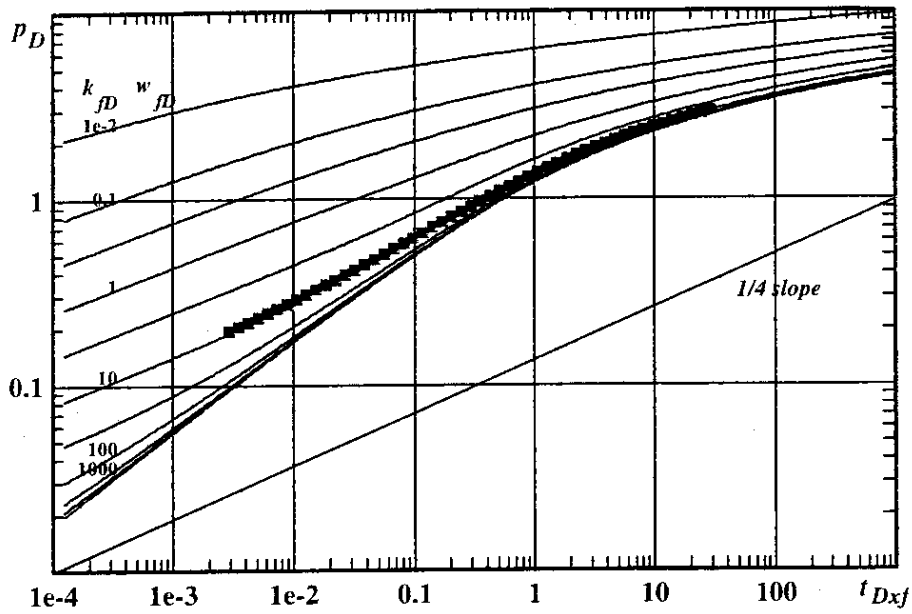

Figure 9: Finite fracture low – Log – Log plot (source R.N. Horne, ref. 5)

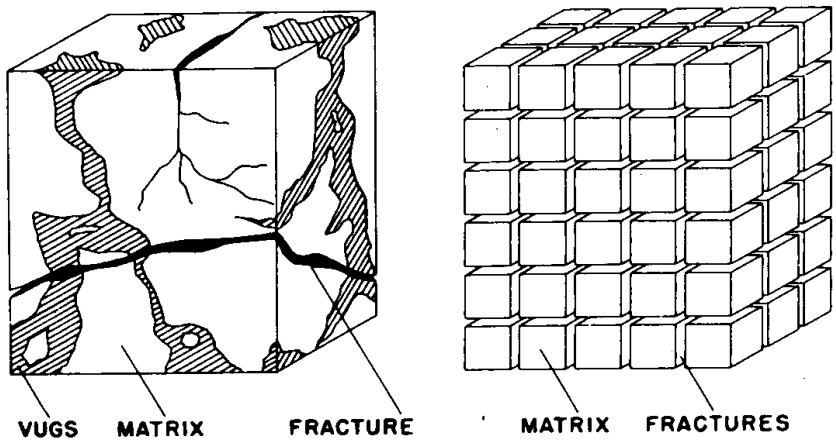

Figure 10: Modelling a naturally fractured reservoir (source: Warren and Root, ref. 4)

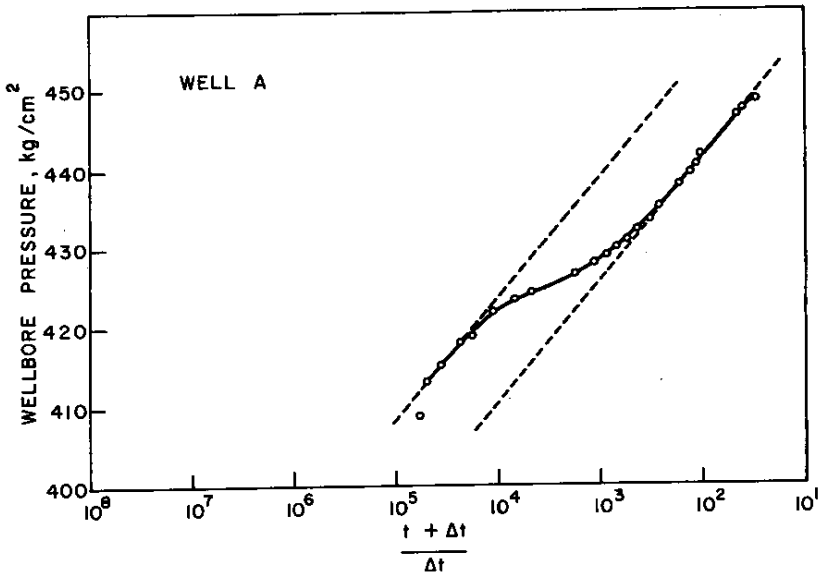

a) Buildup semi-log plot (source: Warren and Root, ref. 4)

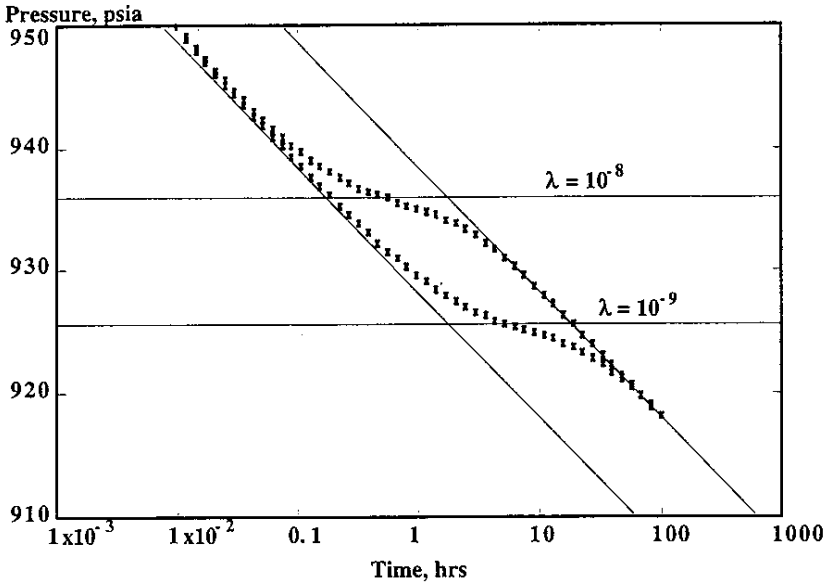

b) Drawdown semi-log plot (source R.N. Horne, ref. 5)

Figure 11: Double porosity responses

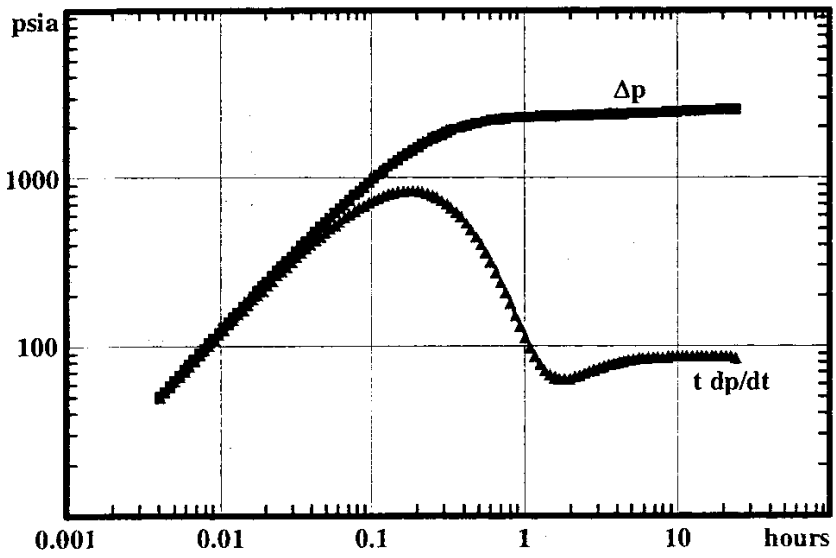

a) Pressure derivative log – log plot

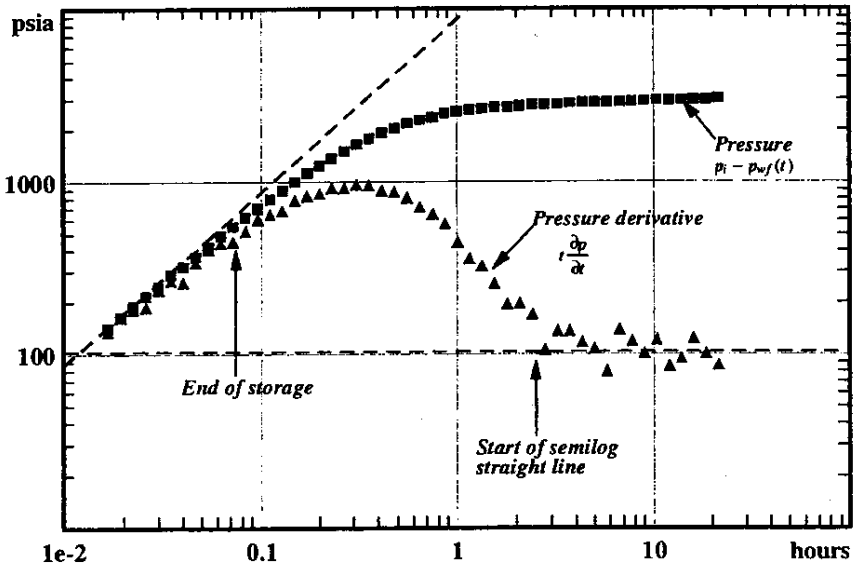

b) Time acting characteristics

Figure 12: Pressure derivative plots (source R.N. Horne, ref. 5)

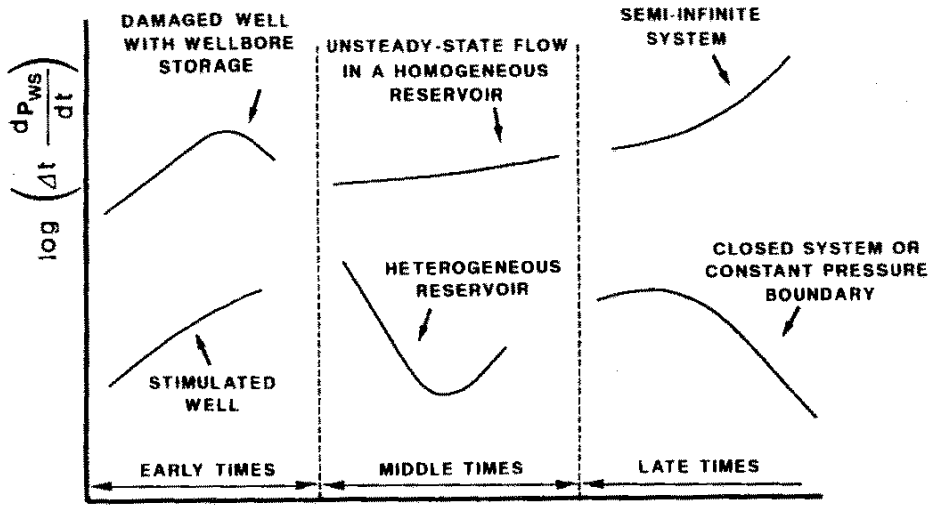

Figure 13: Pressure derivative – Typical signatures (source G.L. Chierici, ref. 7)

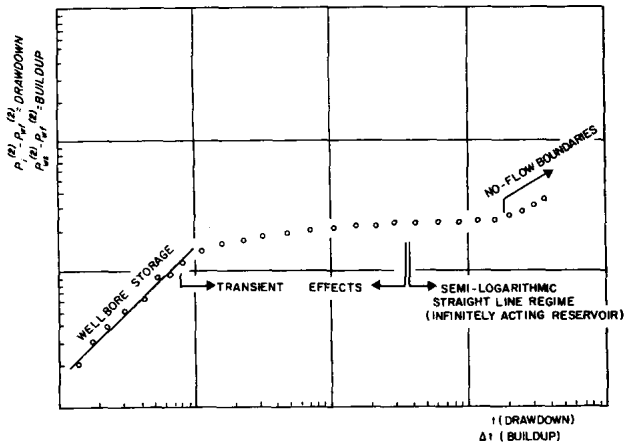

a) Log –log plot pressure buildup and drawdown (source: M.J. Economides, ref. 6)

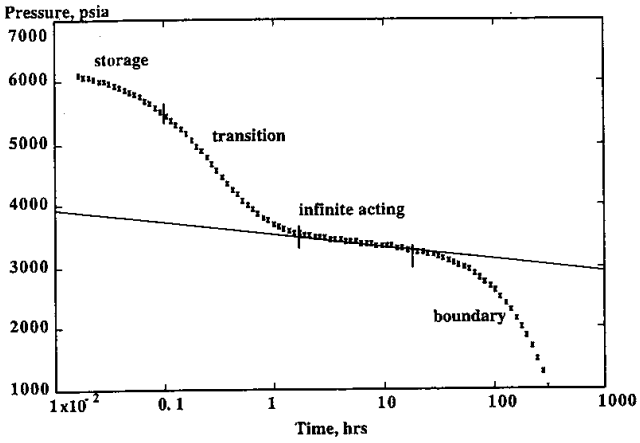

b) Semi-log plot (source: R.N. Horne ref. 5)

	Early time	Intermediate time	Late time
radial flow	storage	infinite acting radial flow	closed boundary sealing fault constant pressure
fractures	storage bilinear flow	radial flow	closed boundary sealing fault constant pressure
dual porosity	storage	dual porosity behaviour transition radial flow	closed boundary sealing fault constant pressure

c) Time diagnostic of flow behaviour (source: R.N. Horne, ref. 5)

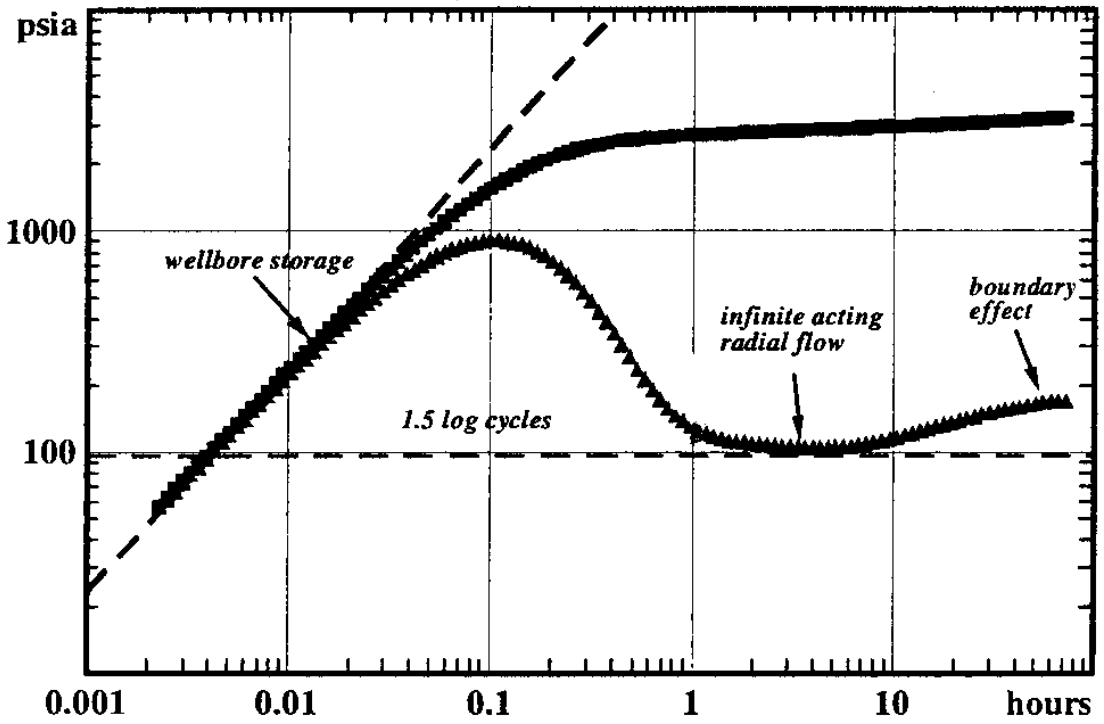

d) Pressure derivative plot

Figure 14: Graphical evaluation of well tests

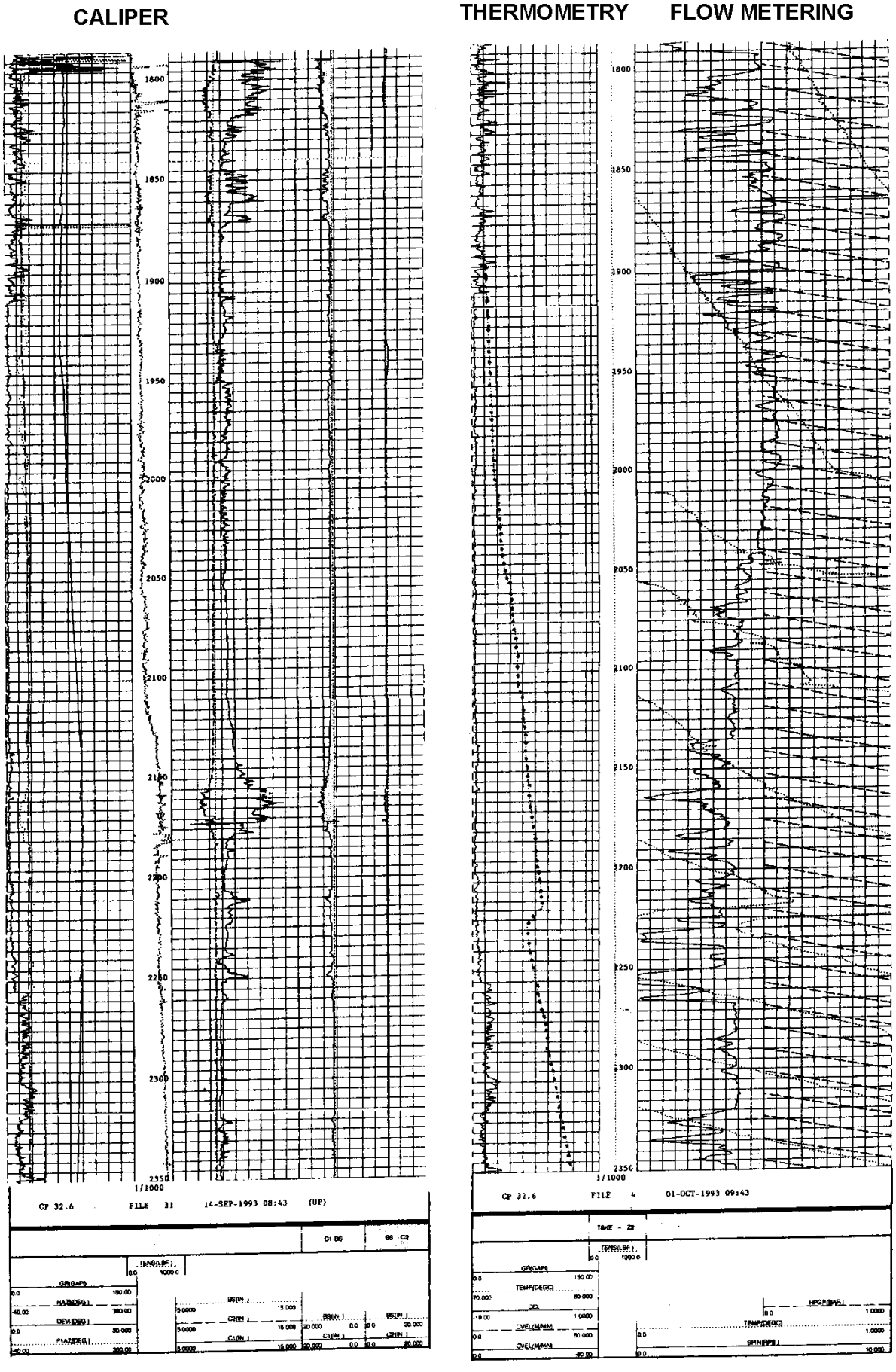

Figure 15: Well production (calliper, thermometry, flow metering) logs (source: GPC and Geologie – Geophysique)

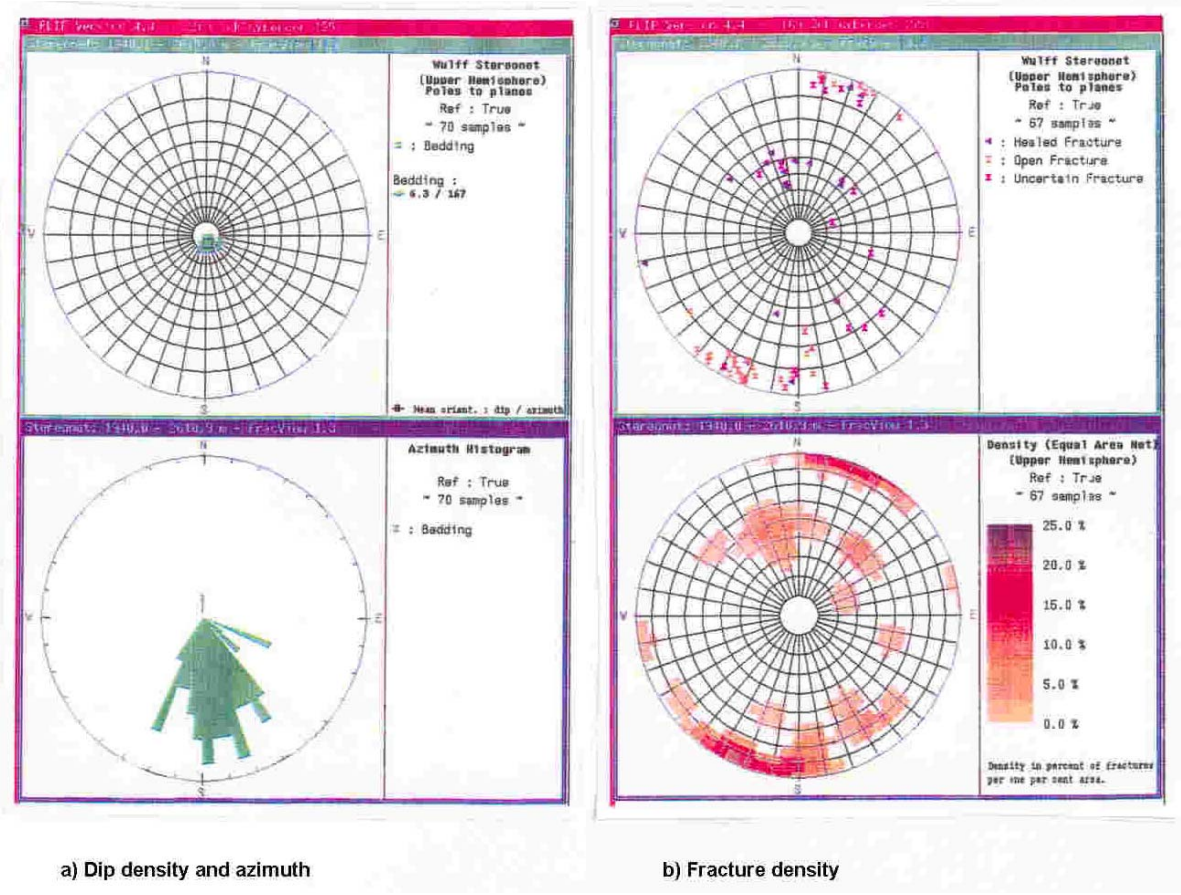

a) Dip density and azimuth

b) Fracture density

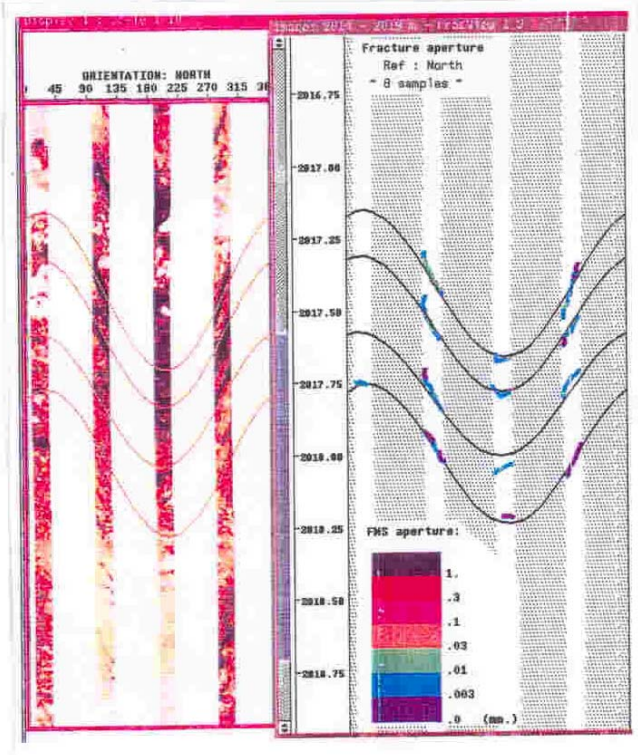

c) Fracture aperture

Figure 16: Fracture analysis. Example of FMS Image processing (source: GPC and Geologie – Geophysique)

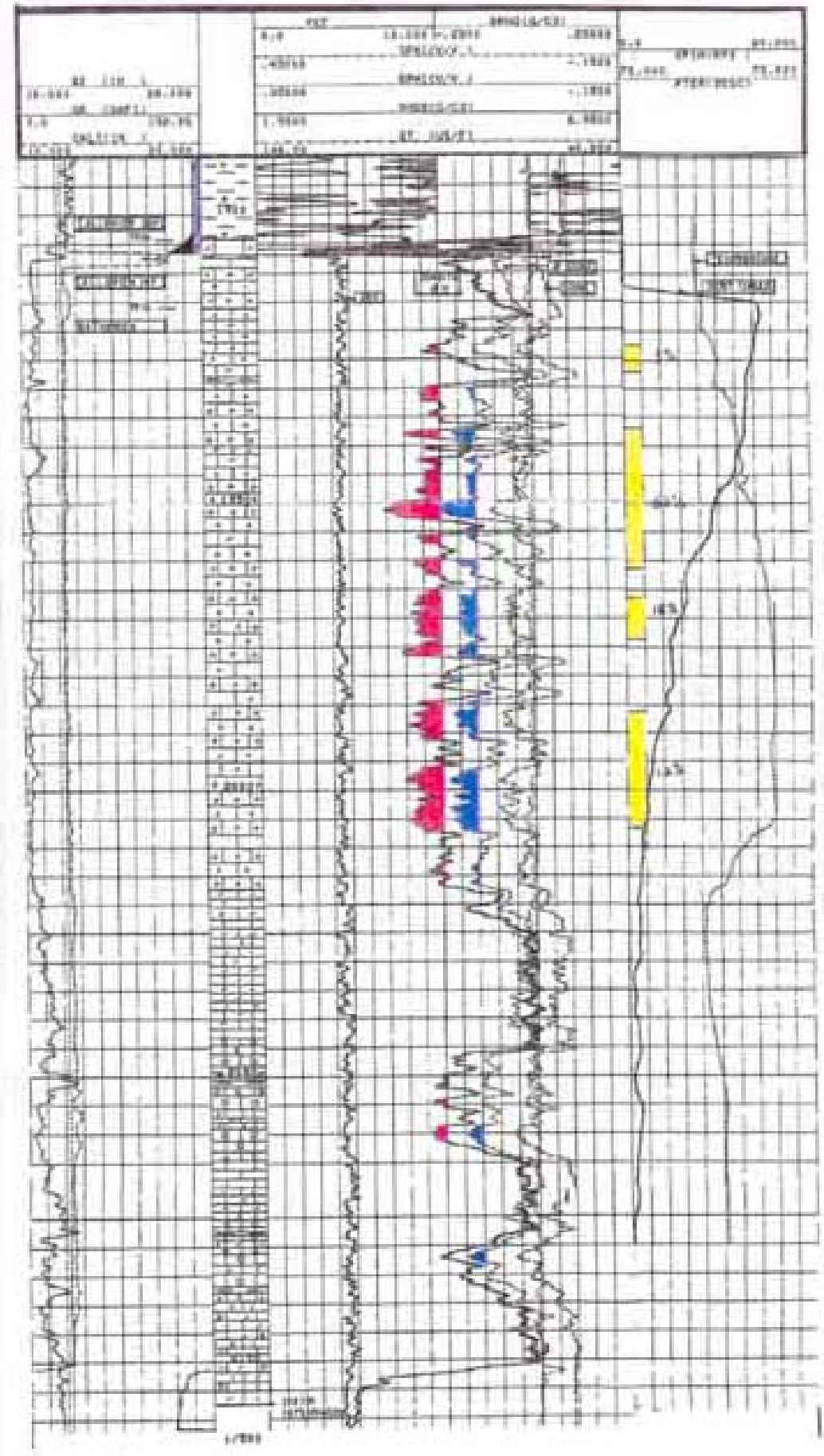

Figure 17: Composite well log – Reservoir analysis
OH porosity/density (BHC, LDL, GR) and production (HRT, Flowmeter) tools (source GPC)

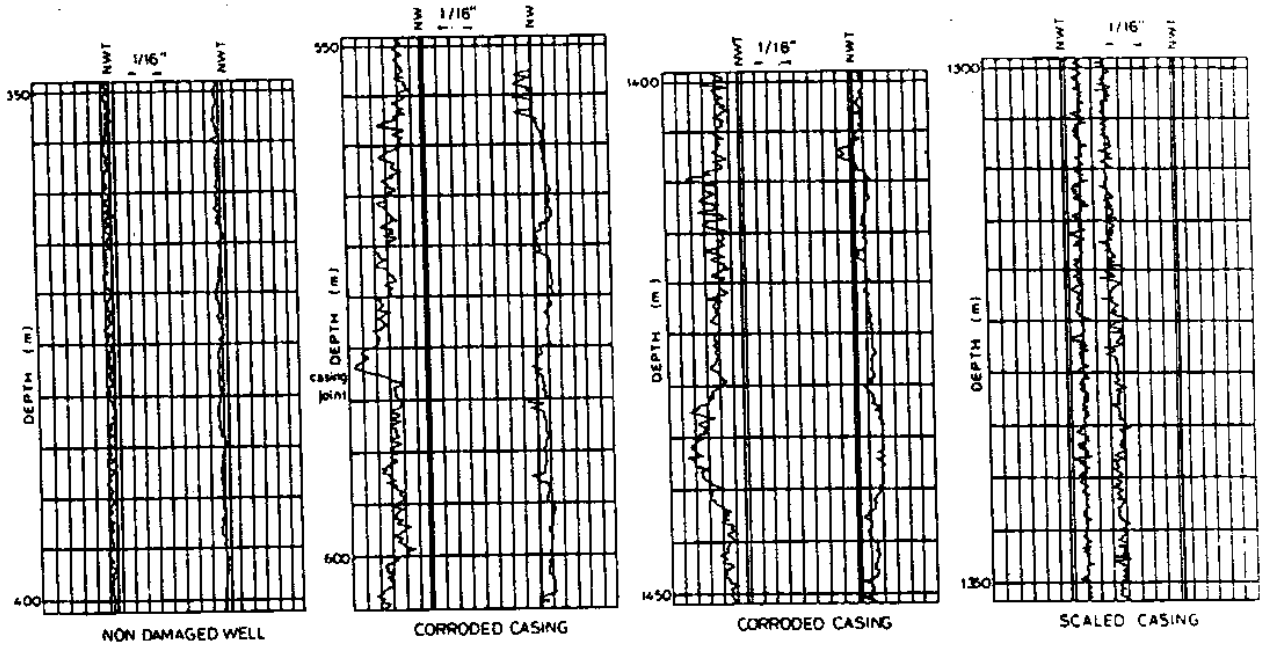

Fig. 18 a) Samples of damaged geothermal wells (7" casings) logged with multifinger callipers (NWT = Nominal Wall Thickness 7" 26 lbs/ft csg) (source: GPC)

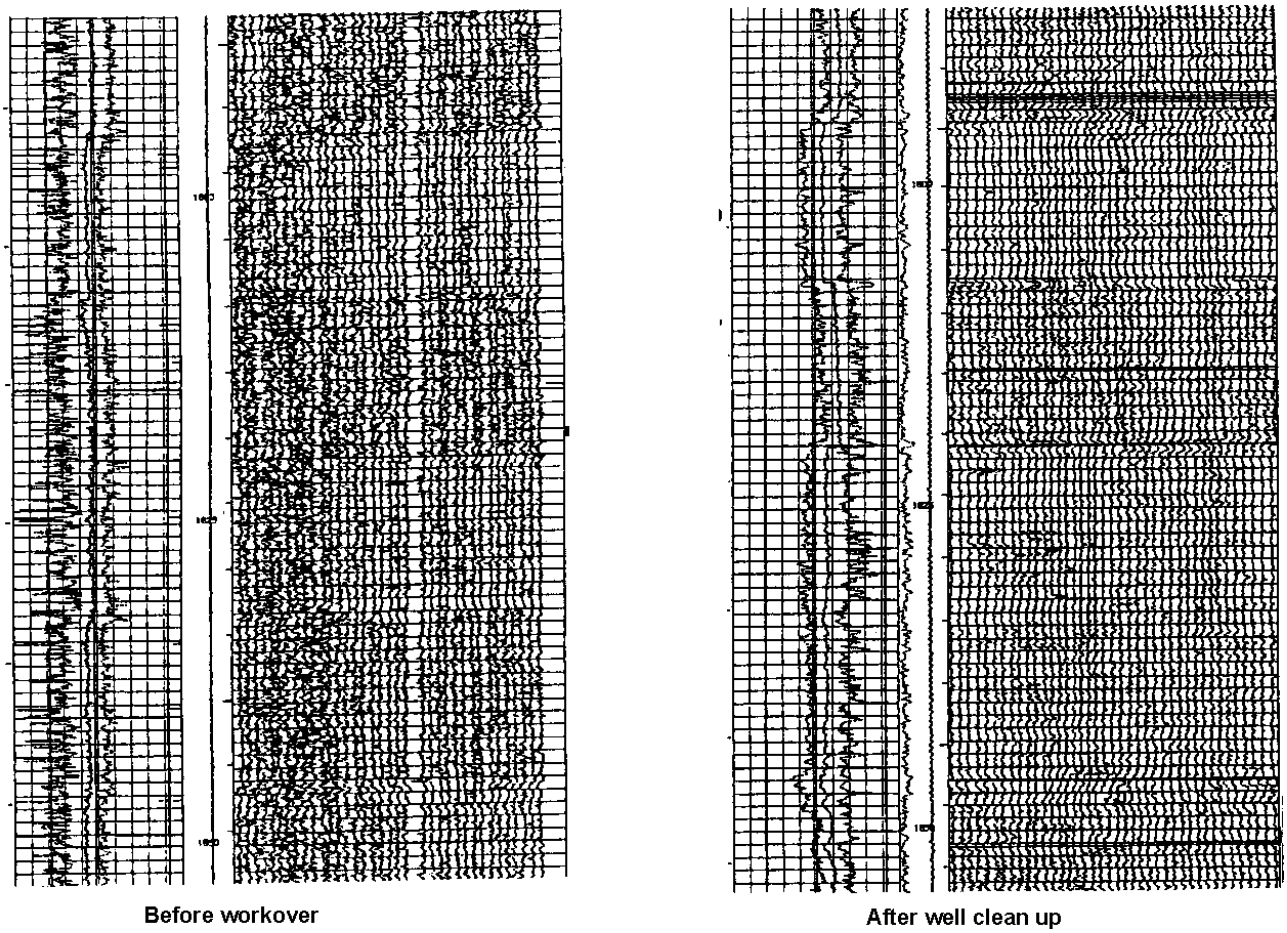

Fig. 18 b) Casing calliper tool. Forty simultaneously recording fingers. Roughness analysis (source: GPC)

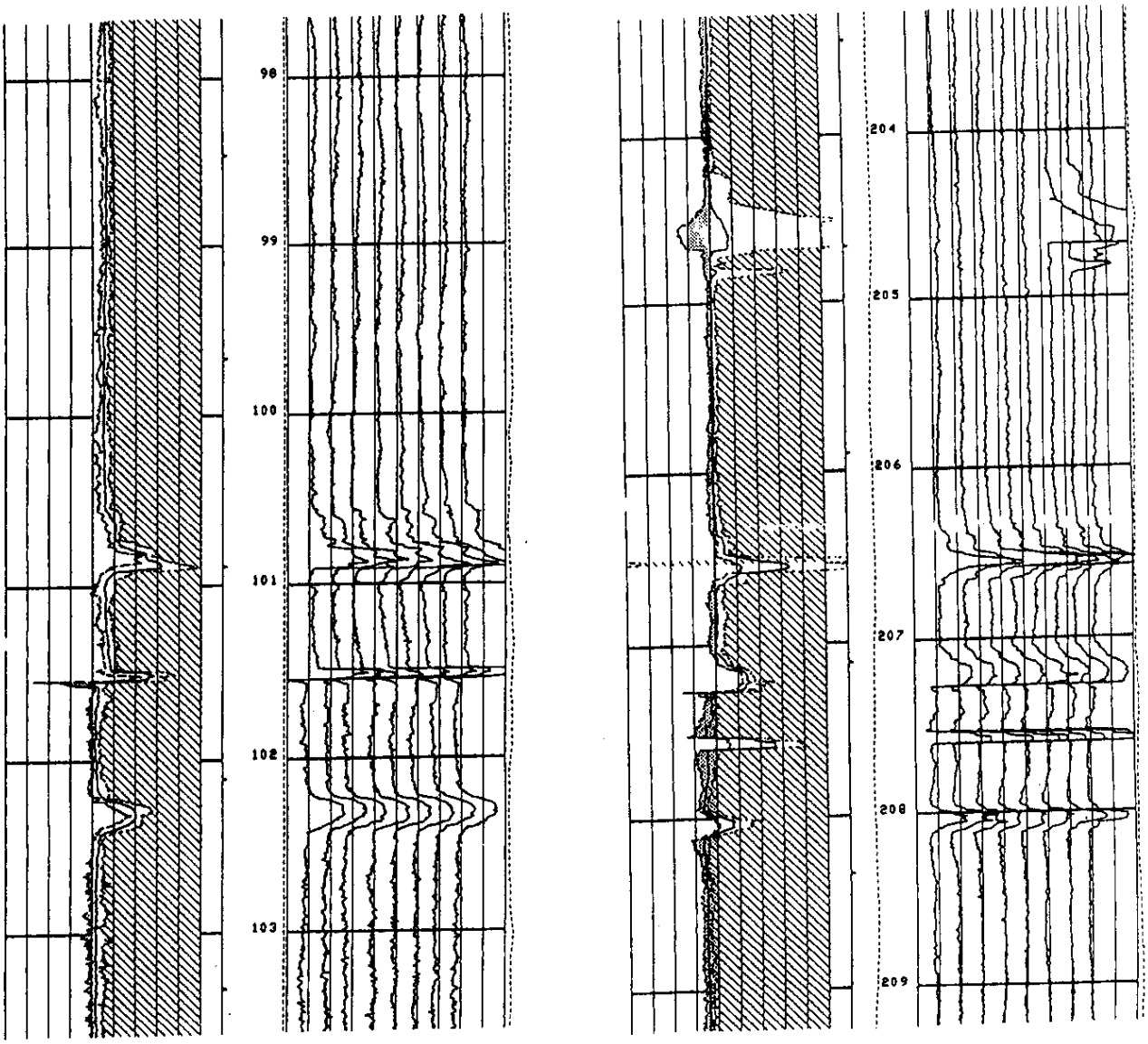

Fig. 18 c) Calliper tool (16 fingers TGS). Evidence of casing damage and piercing (source: GPC)

Figure 18: Examples of casing integrity control by multifinger calliper tools

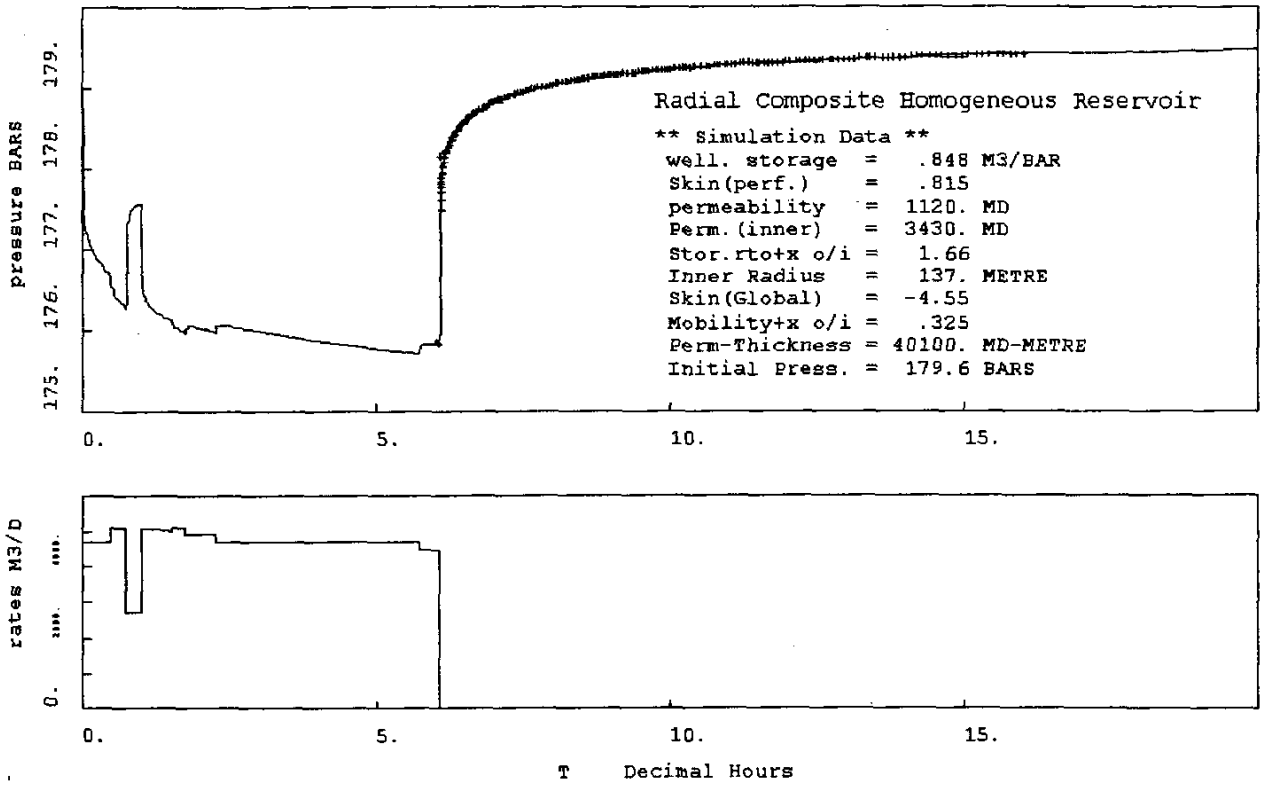

Fig 19 a) Test sequence

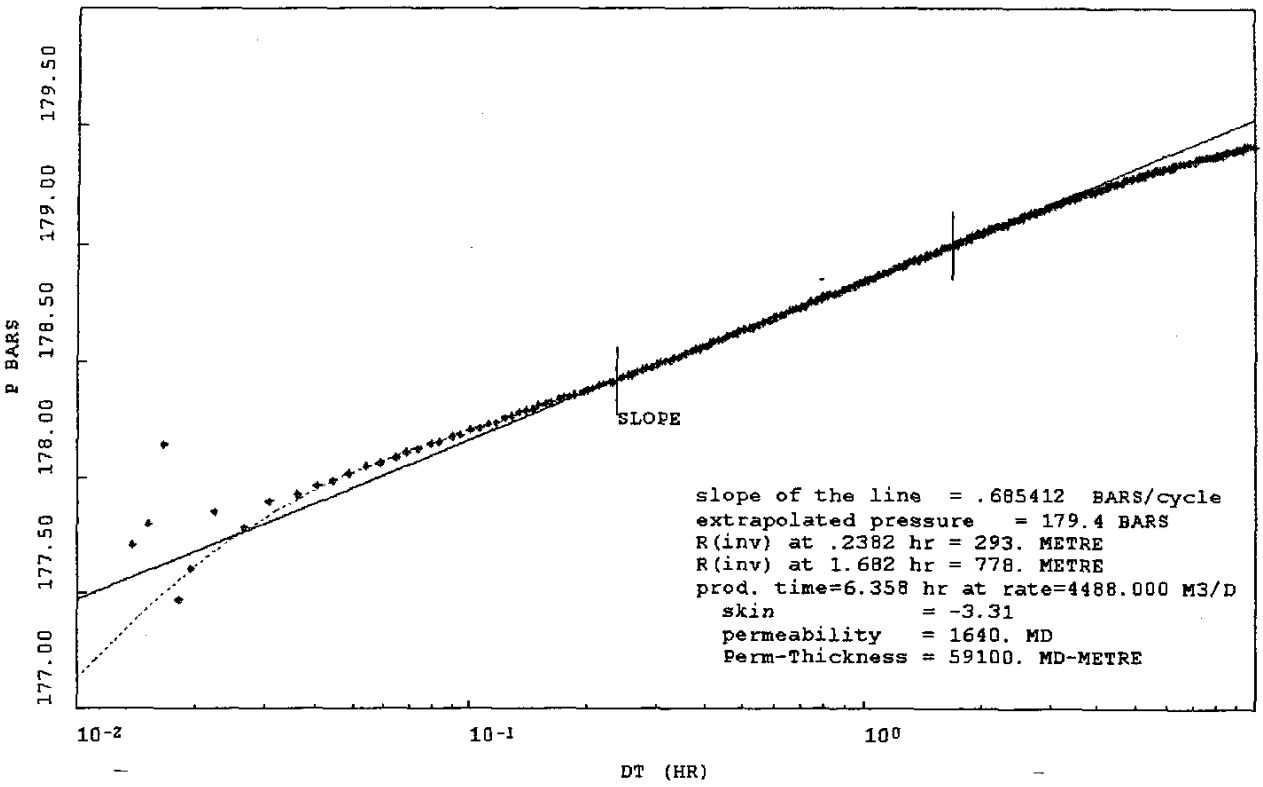

Fig. 19 b) MDH Plot

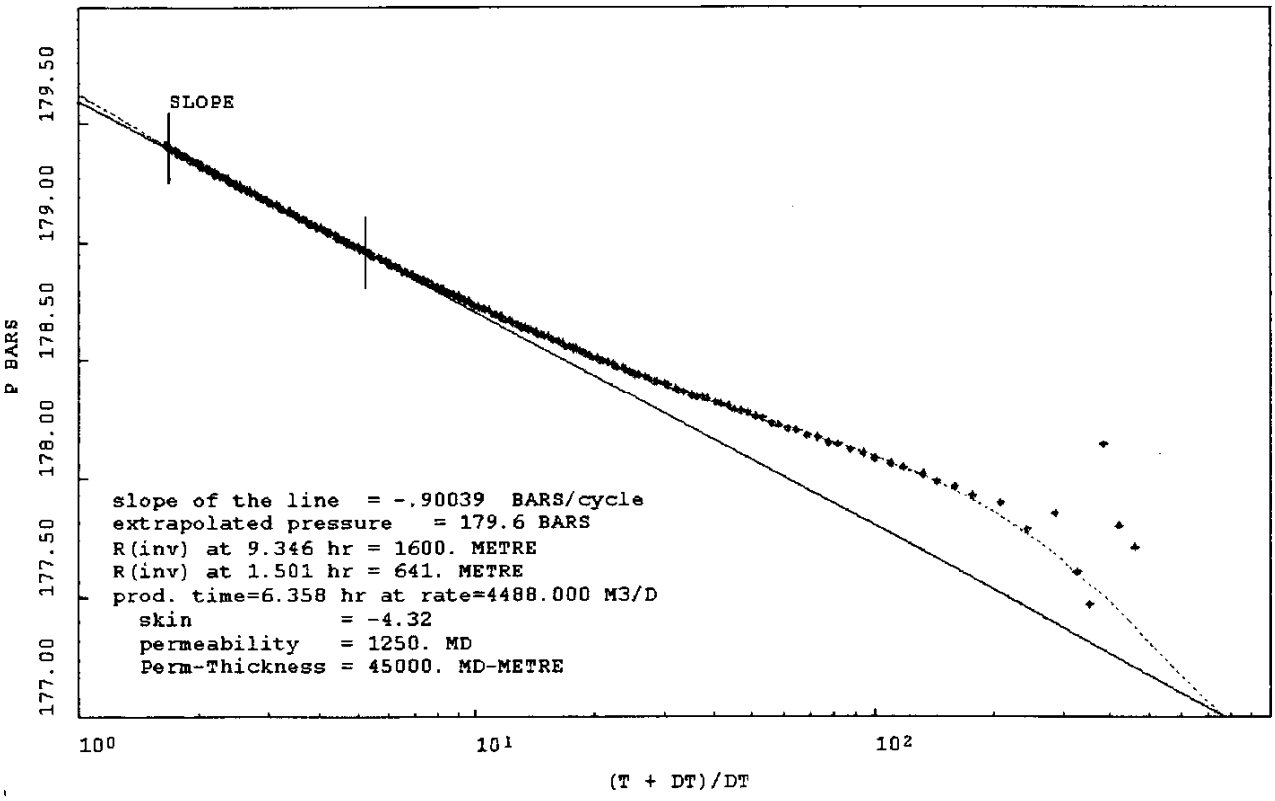

Fig. 19 c) Horner plot

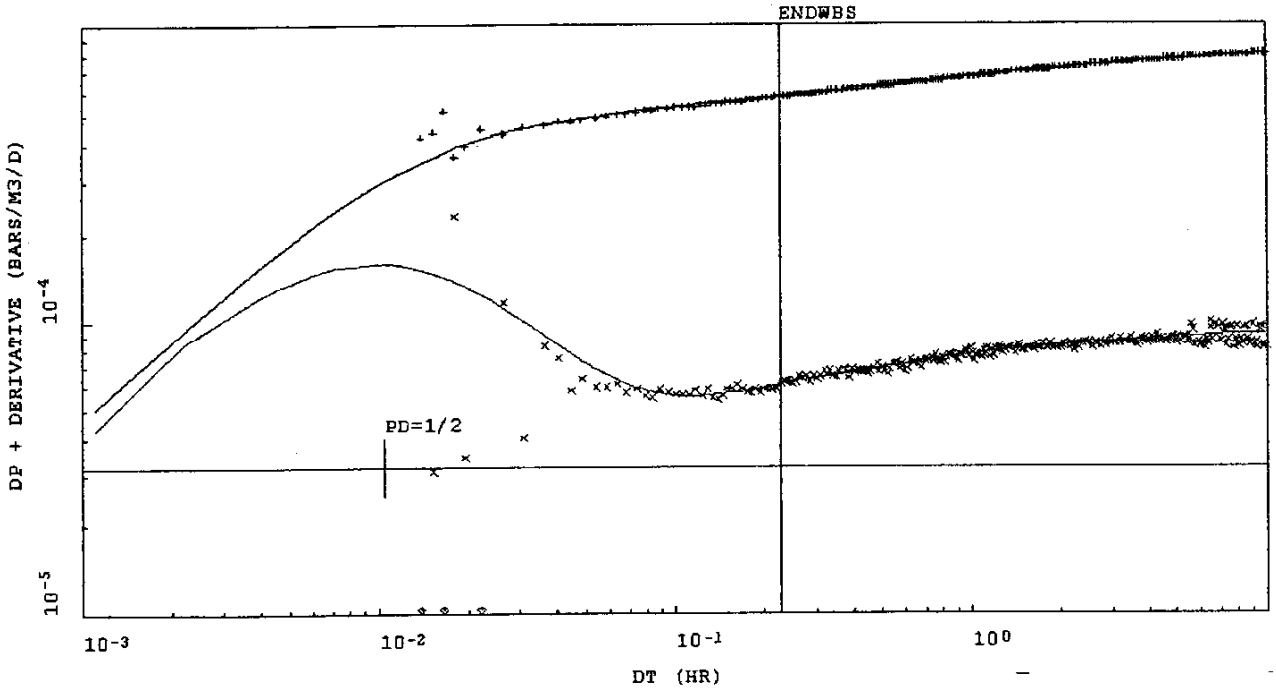

Fig. 19 d) Derivative plot

Figure 19: Pressure buildup test (source: GPC)

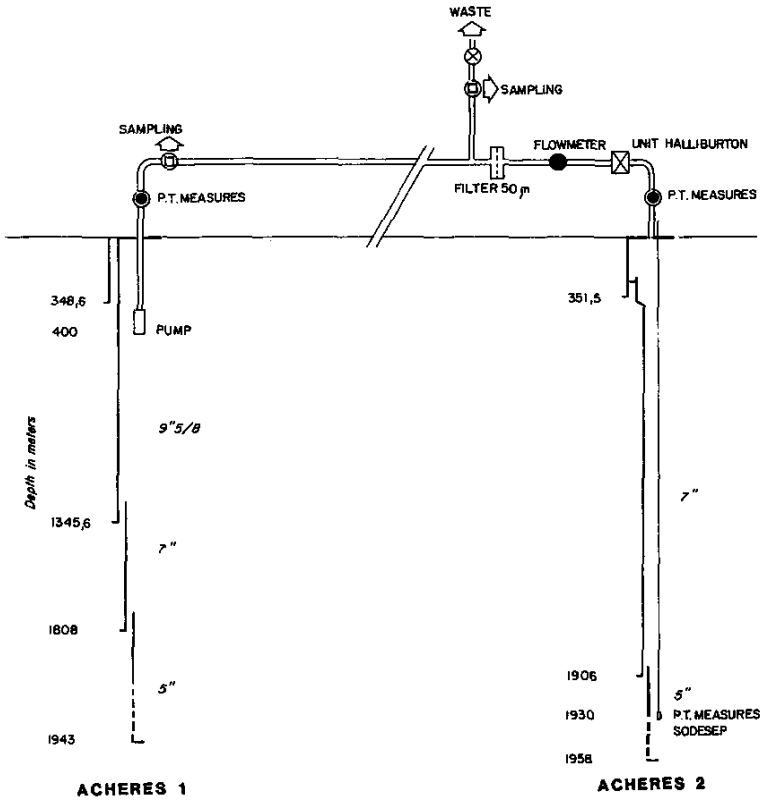

a) Interference and injection test set up

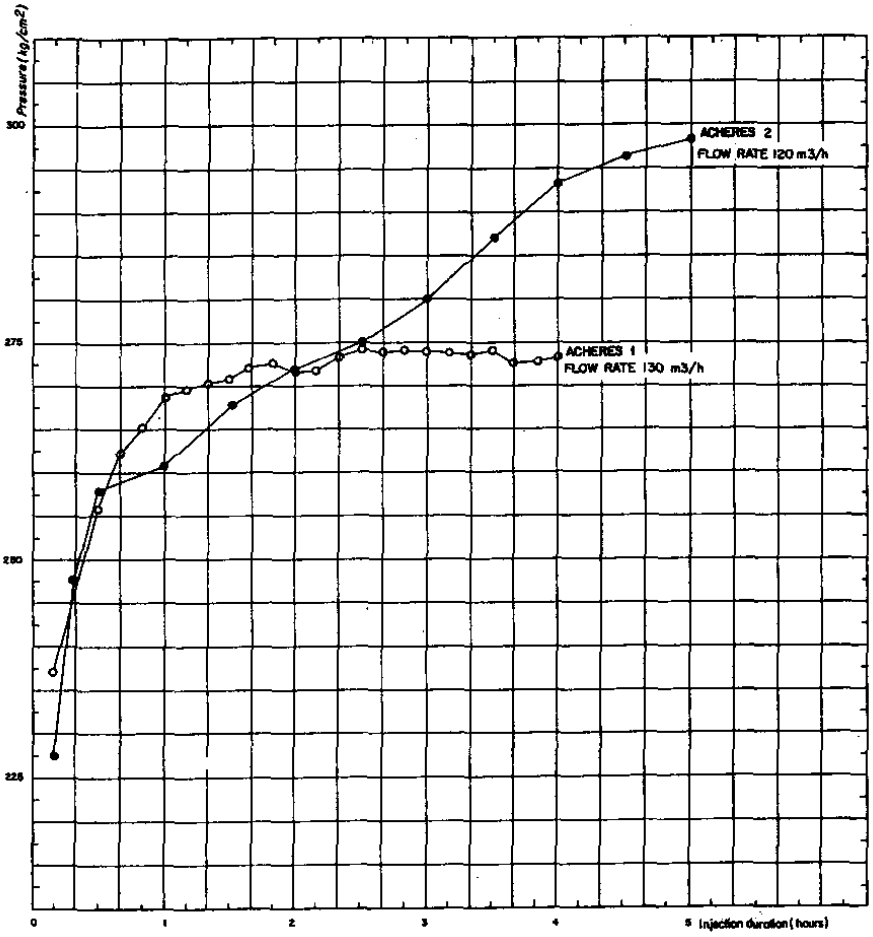

b) Pressure transient responses. Cartesian plot

Figure 20: Injectivity testing (source: P. Ungemach / Geotherma)

SELECTED REFERENCES

1. SCHLUMBERGER (1987). *Log Interpretation Principles/Applications*. Schlumberger Educational Services

2. SCHLUMBERGER (1986). *Log Interpretation Charts*. Schlumberger Well Services.

3. HALLEMBURG, J.K. (1998). *Standard Methods of Geophysical Formation Evaluation*. CRC Press LLC, Levis Publichers – New York – NY.

4. MATTHEWS, C.S. and RUSSELL, D.J. (1967). *Pressure Building and Flow Tests in Wells.* Monograph vol. 1, Heury L. Doherty Series. Soc. of Pet. Eng. Of AIME New York, NY, Dallas, TX.

5. HORNE, R.N. (1995). *Modern Well Test Analysis. A Computer Aided Approach*. 2nd Ed. Petroway, Inc.,Palo Alto, CA.

6. ECONOMIDES, M.J. (1987). *In Engineering Evaluation of Geothermal Reservoirs*. Applied Geothermics, pp. 91-109, Economides, M.J. and Ungemach, P. (edrs). John Wiley and Sons Publ., New York, NY.

7. CHIERICI, G.L. (1994). *Principles of Petroleum Reservoir Engineering.* Vol 1. Springer Verlag Publ., Berlin. Germany.

APPENDIX

Useful charts

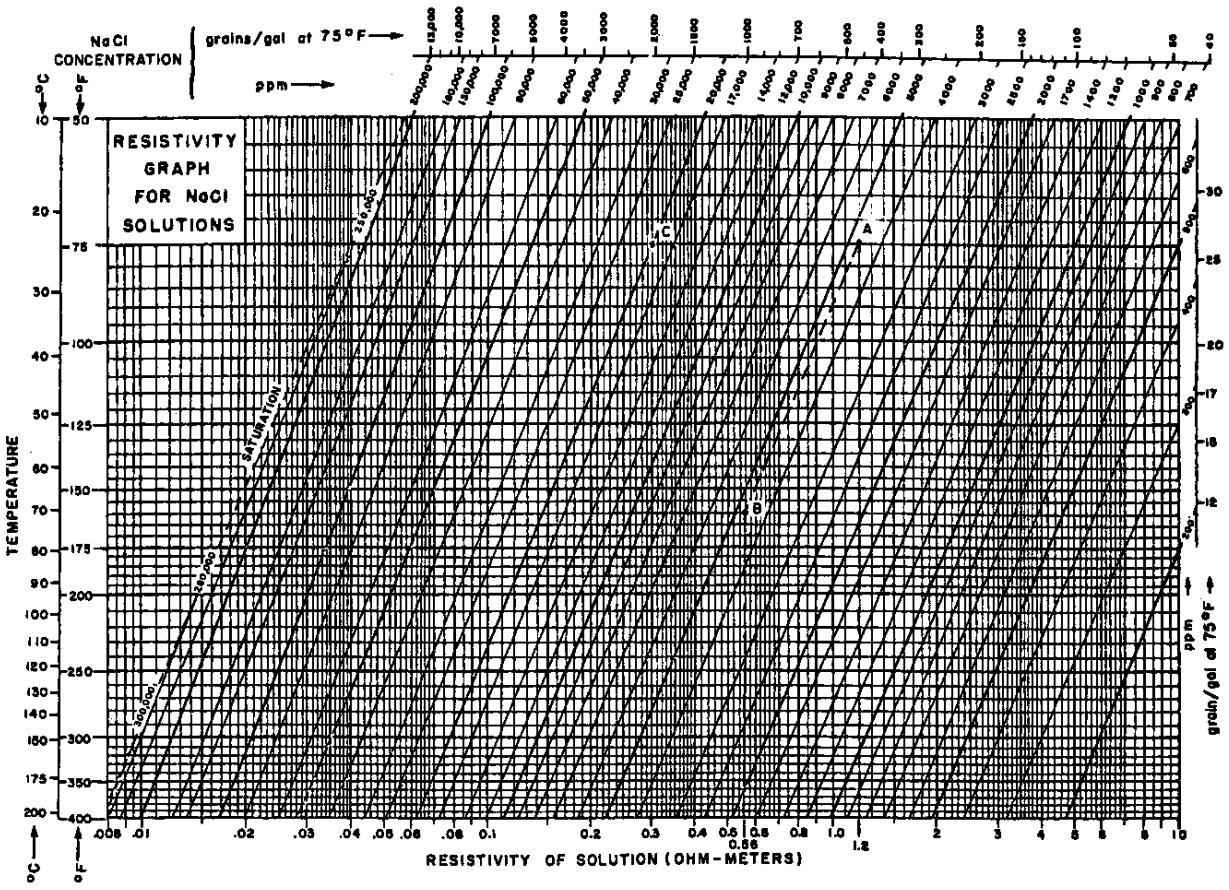

Water resistivity vs salinity and temperature
(source : Schlumberger ref. 2)

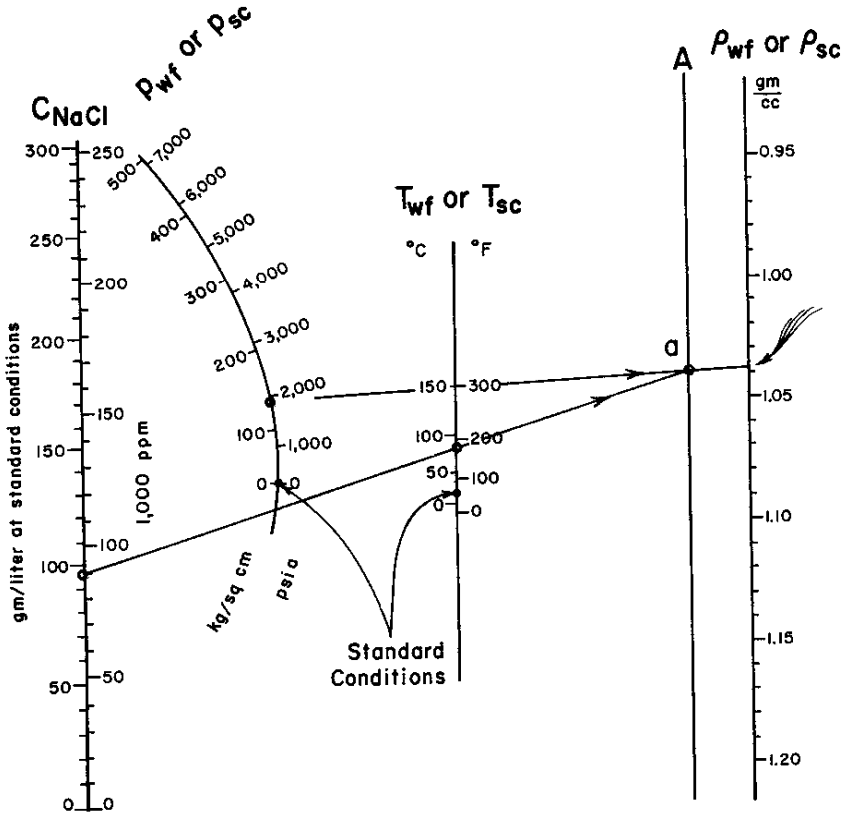

Density of NaCl solutions vs pressure and temperature
(source Schlumberger ref. 2)

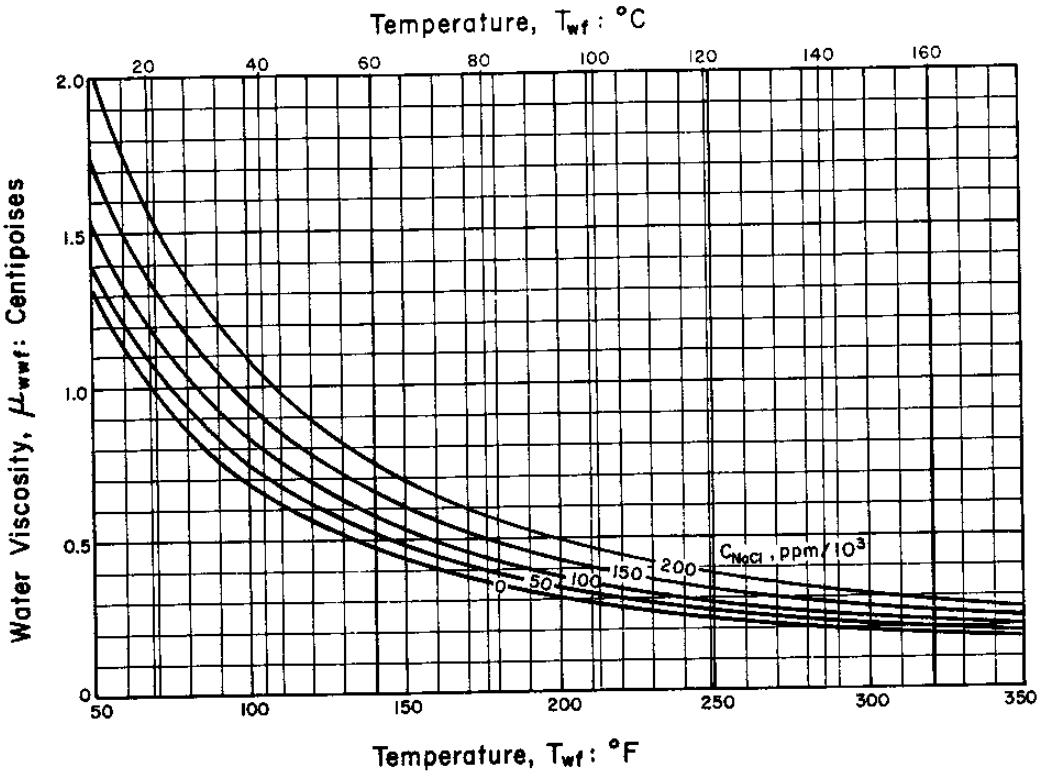

Water viscosity vs temperature and salinity
(source : Schlumberger ref. 2)

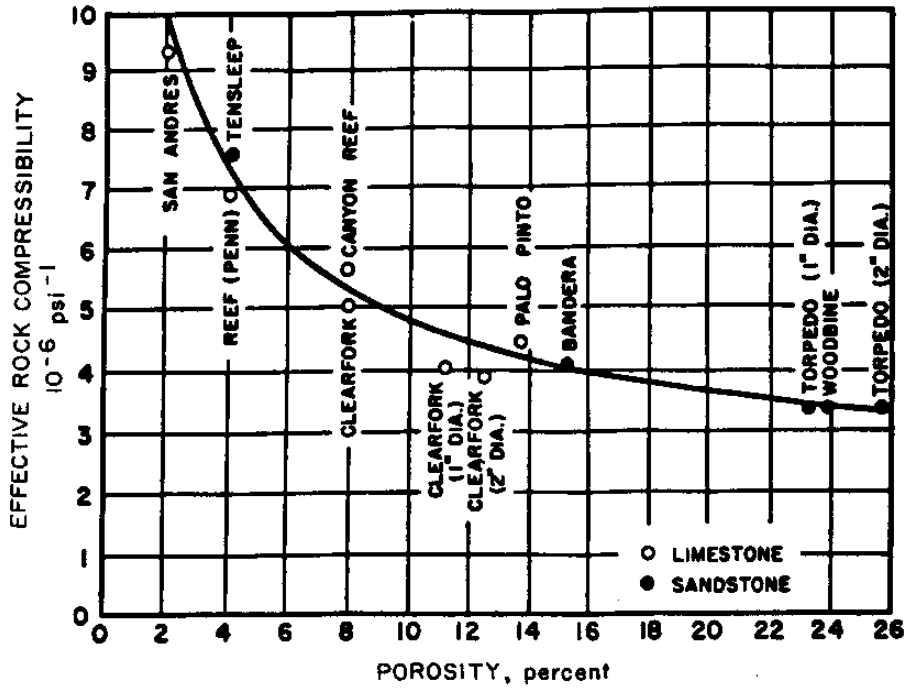

Effective rock compressibility vs porosity
(source : Matthews and Russel ref. 4)